

This is a non peer reviewed preprint submitted to Volcanica

PySulfSat: An Open-Source Python3 Tool for modelling sulfide and sulfate saturation.

Penny E. Wieser and Matthew Gleeson, Earth and Planetary Sciences, UC Berkeley

Please feel free to get in contact with penny_wieser@berkeley.edu with any suggestions. Please, contact me with anything that isn't clear to you, or anything you want added (chances are, if you are confused, or want a model, you are not the only one!).

We will also be adding videos to the YouTube channel:

https://www.youtube.com/channel/UC3J8Lj6Yv_87nvdjjKKcG0g

And there are lots of examples on the Read The Docs page:

https://pysulfsat.readthedocs.io/en/latest/index.html?utm_source=Read+The+Docs

PYSULFSAT: AN OPEN-SOURCE PYTHON3 TOOL FOR MODELING SULFIDE AND SULFATE SATURATION

Penny E. Wieser[‡], Matthew Gleeson[‡]

ABSTRACT

We present PySulfSat, an Open-Source Python3 tool for modeling sulfide and anhydrite saturation in magmas. PySulfSat supports a variety of input data types (spreadsheets, Petrolog3 outputs, MELTS tbl files), and can be directly integrated with alphaMELTS for Python infrastructure to track sulfur solubility during fractional crystallization within a single Jupyter Notebook. PySulfSat allows easy propagation of uncertainty using Monte Carlo methods, and far more customization of calculations than existing tools. For example, the SCSS²⁻ could be calculated with one model using the sulfide composition from a parameterization released with a different SCSS²⁻ model. There are also functions for calculating the proportion of S⁶⁺/S_{Tot} (allowing modeled SCSS and SCAS values to be converted into total S solubility to compare to natural data), and for modeling mantle melting in the presence of sulfides using a variety of SCSS and K_D models. Extensive documentation and worked examples are available at ReadTheDocs (<https://bit.ly/PySulfSatRTD>) along with narrated YouTube videos (<https://bit.ly/PySulfSatYouTube>).

1 INTRODUCTION

Modeling the solubility of sulfur in a silicate melt provides vital insights into the evolution of sulfur and other S-loving (chalcophile) elements during mantle melting and crustal processes such as fractional crystallization and crustal contamination (Ding and Dasgupta [2018]; Wieser et al. [2020]; Reekie et al. [2019]; Muth and Wallace [2022]; Virtanen et al. [2022]; Wieser and Jenner [2021]; Iacono-Marziano et al. [2022]). Modeling the removal of sulfide and sulfate phases is particularly vital to understand the formation of economical deposits of chalcophile elements, as well as the sulfur and metal flux emitted to the atmosphere during volcanic eruptions (Mason et al. [2021]; Edmonds et al. [2018]; Wieser et al. [2020]). A number of different models have been proposed over the years to calculate the sulfide content at sulfide saturation (SCSS²⁻), which describes the amount of sulfide (S²⁻) that can dissolve in a silicate melt saturated in a sulfide phase (e.g., Smythe et al. [2017]; O'Neill [2021]; Fortin et al. [2015]; Li and Ripley [2009]). Numerous models also exist to quantify the sulfate content at anhydrite saturation (SCAS), which describes the amount of sulfate (S⁶⁺) that dissolves in a silicate melt when saturated in anhy-

drite (e.g., Chowdhury and Dasgupta [2019], Zajac and Tsay [2019], Masotta and Keppler [2015], Baker and Moretti [2011], Li and Ripley [2009]). In many magmas with intermediate oxygen fugacity (e.g. in volcanic arcs), S is present as a mixture of S²⁻ and S⁶⁺ species (Muth and Wallace [2021]). O'Neill and Mavrogenes [2022], Nash et al. [2019], and Jugo et al. [2010] produce models to quantify the proportion of these two species as a function of melt redox. These speciation models can be used alongside SCSS²⁻ and SCAS⁶⁺ calculations to obtain the total amount of S that is dissolved in the melt (to compare to measured S contents in volcanic systems).

1.1 Previously-available tools

At the moment, SCSS²⁻ and SCAS⁶⁺ calculations are performed in spreadsheets accompanying each publication (e.g., Smythe et al. [2017]; O'Neill [2021]; Fortin et al. [2015]). These spreadsheets have a limited number of rows for performing calculations (e.g., N=50 for Smythe et al. [2017], N=194 for O'Neill [2021]), making it difficult to apply them to thousands of natural compositions, or outputs of fractional crystallization models with a small temperature step. The prevalence of Excel-based tools also makes it difficult to propagate uncertainty using Monte Carlo methods.

Available tools also make it time consuming and difficult to compare different models. Exist-

^{*}University of California, Berkeley

[‡]Corresponding author: penny_wieser@berkeley.edu

[‡]University of California, Berkeley

ing spreadsheets require users to paste in their melt compositions with oxides in a specific order, and the order differs between spreadsheets. After reformatting the input structure for each model, users would then have to extract outputs and compile these into a single format and location for plotting. There are also tools for which no published spreadsheets exist (e.g. Blanchard et al. [2021]), requiring users to contact the author team to obtain such a tool, or individually interpret the equations (which often contain typos, or ambiguities, particularly regarding which units to use).

The most recent SCSS²⁻ models have a term accounting for the composition of the sulfide (Smythe et al. [2017], O'Neill [2021], Li and Zhang [2022], Blanchard et al. [2021], Liu et al. [2021]), because melts in equilibrium with a sulfide containing Ni and Cu have a substantially lower SCSS compared with melts in equilibrium with pure Fe-S sulfides. However, the spreadsheets for these different models use a variety of approaches to account for the composition of the sulfide, making it hard to directly compare model outputs. The Smythe et al. [2017] Excel workbook has two sheets; one is designed for users to enter a sulfide composition in wt %, while the other sheet calculates a sulfide composition using partition coefficients from Kiseeva and Wood [2015] and an estimate of the Ni and Cu content in the melt. In contrast, the spreadsheet of O'Neill [2021] calculates the Fe/(Fe+Cu+Ni) content of the sulfide using a simple regression based on the FeO_t, Ni and Cu content of the melt (calibrated on MORB), although the user can overwrite this and paste in a fixed value of Fe/(Fe+Cu+Ni). The spreadsheets of Li and Zhang [2022] and Liu et al. [2021] require users to input an estimate of Fe/(Fe+Cu+Ni). To be able to robustly compare the calculated SCSS²⁻ values, it would be preferable to use the same routine for calculating sulfide composition. At the moment, this would require substantial tweaking of spreadsheets by each user.

1.2 PySulfSat: An Open-source approach

The tedium associated with performing SCSS²⁻ and SCAS⁶⁺ calculations in existing spreadsheets, and difficulties associated with comparing models, motivated us to produce PySulfSat. This is an open-source package written in the popular programming language Python3. PySulfSat is designed to be accessible to people with no coding experience. All users must do is install Python on their machine (e.g. through Anaconda). Then, PySulfSat can be installed onto any computer using PyPI (an online software repository) using the following command line prompt:

```
pip install PySulfSat
```

Or, if installation is performed in a Jupyter notebook directly, an explanation mark is added:

```
!pip install PySulfSat
```

Once PySulfSat is installed on a given computer, it must be loaded into each Jupyter Notebook (or other Python file) using any combination of letter users wish (here we use ss):

```
import PySulfSat as ss
```

Any function is then called from PySulfSat using `ss.function_name`.

In addition, we encourage users to import pandas (pandas development team [2020]), NumPy (Harris et al. [2020]), and matplotlib (Hunter [2007]) at the start of each script, for ease of plotting and data manipulation after performing PySulfSat calculations:

```
import pandas as pd
import numpy as np
import matplotlib.pyplot as plt
```

We include numerous narrated worked examples on the PySulfSat YouTube channel to make this package more accessible to non coders (<https://bit.ly/PySulfSatYouTube>). Some relevant terminology for Python and S modeling is shown in Fig. 1.

1.3 Importing data

Users can import data from any excel spreadsheet using the `import_data` function. The input spreadsheet should have the following column headings with oxide contents in wt%:

1. SiO2_Liq
2. TiO2_Liq
3. Al2O3_Liq
4. FeOt_Liq
5. MnO_Liq
6. MgO_Liq
7. CaO_Liq
8. Na2O_Liq
9. K2O_Liq

Certain models also require users to input the following parameters (Fig. 2):

1. P2O5_Liq
2. H2O_Liq

Geological Abbreviations

SCSS	Sulfide content at sulfide saturation
SCAS	Sulfate content at anhydrite saturation
MELTS	A thermodynamic tool for modelling phase equilibrium in magmatic systems
Petrolog3	A popular software tool for modelling fractional crystallization, reverse fractional crystallization, and post-entrapment crystallization corrections of olivine-hosted melt inclusions.

Python Jargon

pandas (pd.)	A Python library allowing handling of spreadsheet-like data structures
pandas Series	A 1D column of data with a column heading. Like a single column in an Excel spreadsheet
pandas DataFrame	A 2D data structure (labelled column headings, rows). Can visualize as a collection of pandas series (like a single sheet in an Excel spreadsheet)
NumPy	A Python library that handles the math used in PySulfSat (e.g., log, exp)
Matplotlib	A Python library used for plotting
String (str)	A piece of text
Float (float)	A single number that is not an integer
Integer (int)	A single number that is an integer

Figure 1: List of abbreviations

3. Fe3Fet_Liq

The `import_data` function returns a pandas dataframe (see Fig. 1). The order of the columns in the input spreadsheet doesn't matter, as columns are identified based on their column heading rather than position. If any column headings are missing in the input spreadsheet, they will be filled with zeros. Any additional columns entered by the user (e.g., temperature, pressure, sulfide composition) are appended onto the end of the outputted dataframe, for easy access for calculations. For example, the O'Neill [2021] and Smythe et al. [2017] models require the Ni and Cu content of the liquid in ppm. These can be stored in a column with any heading the user wishes (e.g. `Ni_Liq_ppm`, `Cu_Liq_ppm`), and then obtained from the outputted dataframe (`df`) using `df['column_name']` to input into the function of interest.

For example, to import generic data (perhaps whole-rock, matrix glass or melt inclusion compositions) from a spreadsheet named "Liquids1.xlsx" stored in "Sheet3":

```
df_out=ss.import_data(filename='Liquids1.xlsx',
sheet_name='Sheet3')
```

This function also supports specific output files from other petrological modelling programs. For example, users can load in the default spreadsheet-based output from Petrolog3.1.1.3 Danyushevsky and Plechov [2011]. Here, the Petrolog output is saved to an excel file named "Petrolog_Mode11.xlsx":

```
df_out=ss.import_data(filename='Petrolog_Mode11.xlsx',
Petrolog=True)
```

Similarly, the standard liquid ".tbl" output from MELTS (Gualda et al. [2012]; Ghiorso and Sack [1995]; Asimow and Ghiorso [1998]) can be imported:

```
df_out=ss.import_data(filename='melts-liquid.tbl',
MELTS=True)
```

In these examples, the `import_data` function has identified the appropriate column headings in each default structure, and has changed the column names into the format required by PySulfSat (e.g., converting `Si02_melt` from Petrolog3 into `Si02_Liq`).

2 UNITS

All temperatures should be entered in Kelvin, all pressures in kbar, and all melt oxides in wt%, apart from Ni and Cu contents in the liquid which are entered in ppm. All ratios are atomic (e.g. $Fe/(Fe+Ni+Cu)$ in the sulfide).

191 2.1 Available functions

192 PySulfSat implements the most recent SCSS²⁻ and
 193 SCAS⁶⁺ models (Fig. 2). The open-source nature of
 194 PySulfSat means we anticipate continuing to add
 195 models as they are published, so users should check
 196 the 'Available Functions' tab at ReadTheDocs.

197 2.2 Calibration datasets

198 Many SCSS and SCAS models are empirical. Thus, it
 199 is not recommended that they are extrapolated too
 200 far beyond the compositional range of the calibra-
 201 tion dataset. We have compiled available calibra-
 202 tion datasets, and incorporated them into PySulf-
 203 Sat (see Fig. 2 for available datasets). This means
 204 that users can easily plot their melt compositions,
 205 and estimates of the pressures and temperatures
 206 of their system alongside the dataset used to cali-
 207 brate each model, to assess its suitability. The func-
 208 tion `return_cali_dataset` returns the calibration
 209 dataset for a given model. For example, to obtain
 210 the calibration dataset for the Smythe et al. [2017]
 211 SCSS model as a pandas.DataFrame:

```
df_S2017=ss.return_cali_datasets(model='S2017_SCSS')
```

212 Fig. 3 shows how these different calibration
 213 datasets can be plotted in TAS space for visual in-
 214 spection.

215 2.3 Worked examples

216 Example Jupyter Notebooks showing a number of
 217 workflows are available at ReadTheDocs page ([bit.ly/PySulfSatRTD](#)). This list is not exhaustive, and
 218 we anticipate that we will continue adding examples
 219 in the future:
 220

- 221 • Notebooks showing how to import different
 222 data types (e.g. measured oxide contents,
 223 Petrolog3 files, and MELTS tbl outputs).
- 224 • Notebooks showing how to calculate the SCSS
 225 and SCAS using a variety of models during
 226 fractional crystallization from a Petrolog3 out-
 227 put (Danyushevsky and Plechov [2011]). This
 228 example also shows how to calculate the tra-
 229 jectory of S if a sulfide phase wasn't present,
 230 and how to calculate the mass fraction of sul-
 231 fide which has formed during crystallization.
- 232 • Notebooks showing how to run a MELTS frac-
 233 tional crystallization paths at a single pressure
 234 and at multiple pressures using PyMELTScalc
 235 (Gleeson et al. [2023]), and then calculate the
 236 SCSS and SCAS within the same Jupyter Note-
 237 book.
- 238 • Notebooks showing how to model the SCSS
 239 from a Petrolog3 path, and compare models of

S contents and sulfide composition to natural
 melt inclusion and sulfide data.

- Notebooks showing how to calculate the pro-
 portion of S⁶⁺ using the models of Jugo et al.
 [2010], Nash et al. [2019], and O'Neill and
 Mavrogenes [2022].
- Notebooks showing how to perform calcula-
 tions of trace element evolution during mantle
 melting in the presence of sulfide using differ-
 ent SCSS, SCAS and K_D models.
- Notebooks showing how to propagate uncer-
 tainty in input parameters using Monte Carlo
 methods to obtain 1σ errors for different cal-
 culations.
- Notebooks showing other useful features, in-
 cluding calculating K_Ds using various mod-
 els, converting between S isotope ratios and
 delta notation, and abundances of different S-
 bearing species.

3 SCSS²⁻ MODELS

There are a number of ways to perform SCSS cal-
 culations, with various options discussed below
 (worked examples are available at ReadTheDocs).

3.1 Using measured sulfide compositions

The newest SCSS models (e.g., O'Neill [2021],
 Smythe et al. [2017], Li and Zhang [2022], Blan-
 chard et al. [2021]) contain terms for the composi-
 tion of the sulfide. In some situations, the sulfide
 composition may have been directly measured in
 the samples of interest (e.g. using Energy Disper-
 sive Spectroscopy, Wieser et al. [2020]). If so, the
 function `calculate_sulf_FeFeNiCu` can be used to
 convert measured elemental abundances in wt%
 into the atomic Fe/(Fe+Ni+Cu) ratio used by SCSS
 models. In some systems, the Fe/(Fe+Ni+Cu) may
 remain approximately constant during fractional
 crystallization (Wieser et al. [2020]), meaning that
 a fixed value for this ratio can be used for sim-
 plicity. Figure 4 shows a worked example calculat-
 ing the SCSS²⁻ using the models of Smythe et al.
 [2017], O'Neill [2021] and Li and Zhang [2022] for
 Fe/(Fe+Ni+Cu)=0.65. The expected increase in the
 S content of the melt with fractional crystallization
 in the absence of a S-bearing phase is also calculated
 using the function `crystallize_S_incomp` for com-
 parison (black dashes), and these different S trajec-
 tories are plotted using matplotlib (where they can
 be compared to natural melt inclusion or quenched
 submarine glass data).

Reference	Name in PySulfSat	Melt composition?	T-sens?	P-sens?	H ₂ O-sens?	Fe ³⁺ sensitive?	Sulfide/Sulfate comp?	Call dataset available?
SCAS models								
Chowdhury & Dasgupta (2019)	"calculate_CD2019_SCAS"	✓	✓	✗	✓	✗	✗	✓
Zajacz & Tsay (2019)	"calculate_ZT2022_SCAS"	✓	✓	✗	✓	✗	✗	✓
Masotta & Keppler (2015)	"calculate_MK2015_SCAS"	✓	✓	✗	✓	✗	✗	✓
SCSS models								
Li and Zhang (2022)	"calculate_LiZhang2022_SCSS"	✓	✓	✓	✓	✓	✓	✓
Blanchard et al. (2021)	"calculate_B2021_SCSS"	✓	✓	✓	✓	✗	✓	✓
O'Neill (2021)	"calculate_O2021_SCSS"	✓	✓	✓	✗	✓	✓	
O'Neill and Mavrogenes (2022) ¹	"calculate_OM2022_SCSS"	✓	✓	✓	✗	✓	✓	✓
Liu et al. (2021)	"calculate_Liu2021_SCSS"	✗	✓	✓	✓	✗	✓	✓
Smythe et al. (2017)	"calculate_S2017_SCSS"	✓	✓	✓	✓	✓	✓	✓
Fortin et al. (2015)	"calculate_F2015_SCSS"	✓	✓	✓	✓	✗	✗	✓
Sulfide composition models								
O'Neill (2021)	"Calc_ONeill"	✓	✗	✗	✗	✓		
Smythe et al. (2017) using Kiseeva et al. (2015)	"Calc_Smythe"	✓	✓	✗	✗	✓		

Calculating Proportion of S⁶⁺ using empirical approaches

Reference	Name in PySulfSat	Input parameters
Jugo et al. (2010)	"calculate_S6St_Jugo2010_eq10"	ΔQFM
Nash et al. (2019)	"calculate_S6St_Nash2019"	T, Fe ³⁺ /Fe _T
O'Neill and Mavrogenes (2022)	"calculate_OM2022_S6St"	Melt comp, T, log(<i>f</i> _{O₂}) or Fe ₃ /Fe _T

Correcting SCSS²⁻ and SCAS⁶⁺ calculations for S_T

Name in PySulfSat	Input arguments
"calculate_SCSS_Total"	SCSS ²⁻ , S ⁶⁺ /S _T
"Calculate_SCAS_Total"	SCAS ⁶⁺ , S ²⁻ /S _T
"Calculate_S_Total_SCSS_SCAS"	SCSS ²⁻ , SCAS ⁶⁺ , S ⁶⁺ /S _T , or model ('Nash', 'Jugo' or 'Kleinsasser')

Other functions

"crystallize_S_incomp"	Calculates S left in the melt for a given F_melt (assuming S is entirely incompatible)
"calculate_mass_frac_sulf"	Calculates mass fraction of sulfide removed for a fractional crystallization path where the SCSS is modelled
"convert_d34_to_3432S"	Converts δ ³⁴ S to ³⁴ S/ ³² S
"Lee_Wieser_sulfide_melting"	Modelling of S and chalcophile element behaviour during mantle melting.
For Monte Carlo simulations	
'add_noise_2_dataframes'	Generate duplicated rows in df1 based on errors present in df2
'add_noise_series', 'duplicate_dataframe'	Used to simulate uncertainty in specific variables
'av_noise_samples_series'	Average outputs from Monte Carlo simulations per sample

Figure 2: Models currently available in PySulfSat. SCAS⁶⁺ models: [Chowdhury and Dasgupta \[2019\]](#), [Zajacz and Tsay \[2019\]](#) and [Masotta and Keppler \[2015\]](#). SCSS²⁻ models: [Li and Zhang \[2022\]](#), [Blanchard et al. \[2021\]](#), [O'Neill \[2021\]](#), [O'Neill and Mavrogenes \[2022\]](#), [Liu et al. \[2021\]](#), [Smythe et al. \[2017\]](#) and [Fortin et al. \[2015\]](#). The SCSS model of [O'Neill \[2021\]](#) and [O'Neill and Mavrogenes \[2022\]](#) are extremely similar, differing only with regard to a 7.2*Fe*Si term in 2021, and a 7.2*(Mn+Fe)*Si term in 2022. S⁶⁺ corrections from [Jugo et al. \[2010\]](#), [Nash et al. \[2019\]](#) and [O'Neill and Mavrogenes \[2022\]](#). We suggest readers check the ReadTheDocs page for a complete list as we will add new models as they become available.

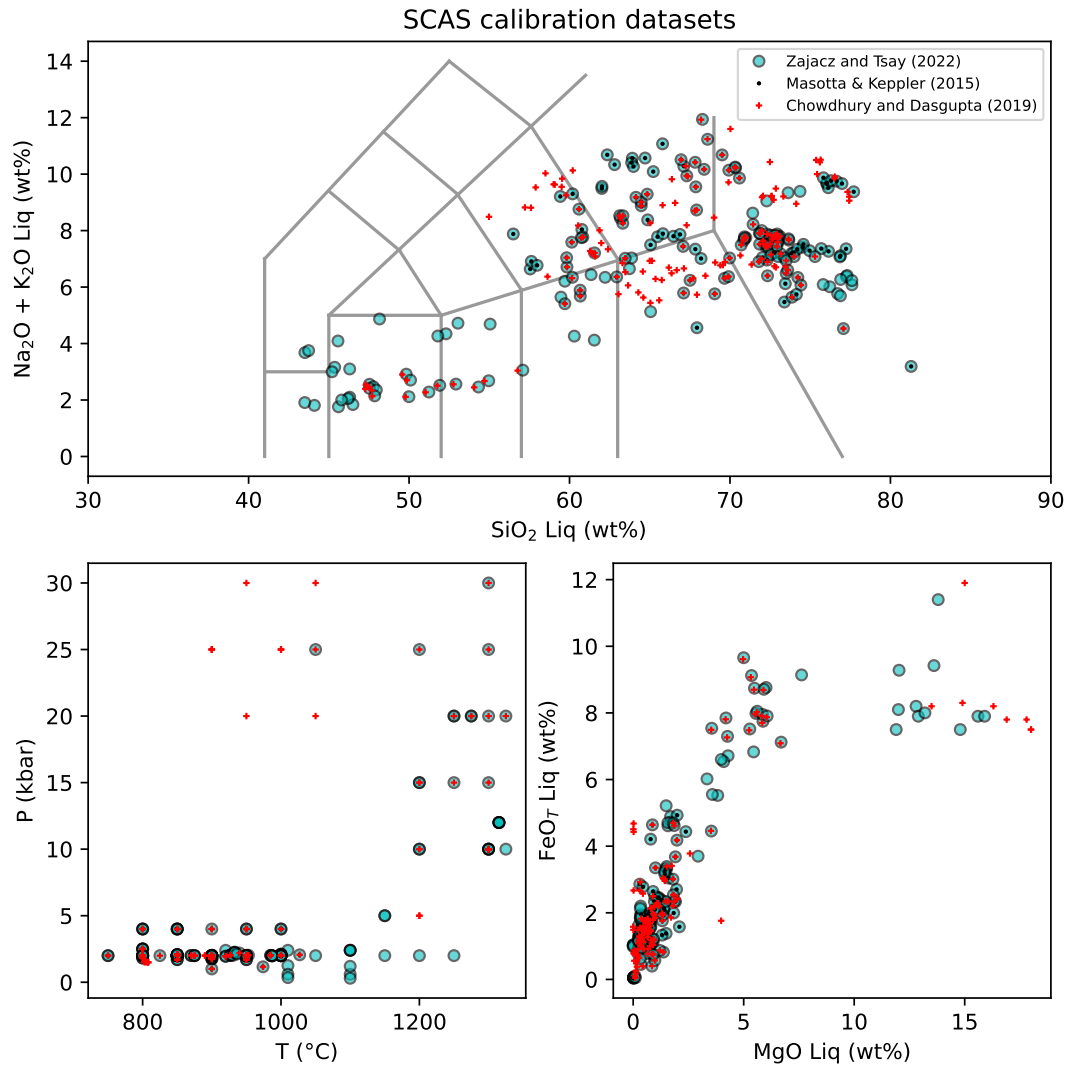


Figure 3: Plots of SCAS calibration datasets in P-T-X space. An example notebook to produce these plots and overlay user data is available at ReadTheDocs. Similar plots can easily be made for SCSS models.

Load data from a Petrolog3 output file

	A	B	C	D	E	F	G	H	I	J	AY	AZ	BA
1	SiO2_ma	TiO2_ma	Al2O3_ma	Fe2O3_ma	FeO_ma	MnO_ma	MgO_ma	CaO_ma	Na2O_ma	K2O_ma	density	Ln(viscosit	Melt_%_r
2	49.901	0.9981	14.9715	0.9839	8.0964	0.0998	9.9763	11.9772	2.4953	0.1996	2.683	6.25	99.99
3	49.9978	1.0081	15.122	0.9743	8.0754	0.1008	9.6064	12.0976	2.5203	0.2016	2.682	6.38	98.995
4	50.0982	1.0185	15.277	0.9649	8.0492	0.1018	9.2279	12.2216	2.5462	0.2037	2.681	6.52	97.9904
5	50.2003	1.0289	15.4337	0.9561	8.0178	0.1029	8.8486	12.3469	2.5723	0.2058	2.68	6.67	96.9959

```
df_out=ss.import_data('PetrologCalculations.xlsx', Petrolog=True)
df_out.head()
```

Specifying this is a Petrolog3 file prints reformatted data for inspection

We have replaced all missing liquid oxides and strings with zeros.

	SiO2_Liq	TiO2_Liq	Al2O3_Liq	FeOt_Liq	MnO_Liq	MgO_Liq	CaO_Liq	Na2O_Liq	K2O_Liq	P2O5_Liq	H2O_Liq	Fe3Fet_Liq
0	49.9010	0.9981	14.9715	8.981890	0.0998	9.9763	11.9772	2.4953	0.1996	0.0998	0.0	0.098586
1	49.9978	1.0081	15.1220	8.952251	0.1008	9.6064	12.0976	2.5203	0.2016	0.1008	0.0	0.097947
2	50.0982	1.0185	15.2770	8.917591	0.1018	9.2279	12.2216	2.5462	0.2037	0.1018	0.0	0.097380

Option 1: Calculate Smythe et al. (2017) SCSS (measured sulf comp)

```
Smythe_FixedSulf=ss.calculate_S2017_SCSS(df=df_out,
T_K=df_out['T_K'], P_kbar=df_out['P_kbar'],
Fe3Fet_Liq=df_out['Fe3Fet_Liq'],
Fe_FeNiCu_Sulf=0.65)
Smythe_FixedSulf.head()
```

Reading melt composition, T, P from dataframe extracted from Petrolog3
Measured sulfide composition
Inspect calculations

Using inputted Fe_FeNiCu_Sulf ratio for calculations.

You havent entered a value for Ni_FeNiCu_Sulf and Cu_FeNiCu_Sulf so we cant calculate the non-ideal SCSS

	SCSS_ideal_ppm_Smythe2017	SCSS_ideal_ppm_Smythe2017_1sigma	Si_XA_ideal	Ti_XA_ideal	Al_XA_ideal	Mg_XA_ideal	
0	1163.723704		317.894143	-12643.824134	-77.425187	-2992.932034	-1910.028590
1	1132.276539		309.303728	-12681.503374	-78.282101	-3026.156769	-1841.118249
2	1099.610160		300.380260	-12720.419296	-79.173410	-3060.410799	-1770.448728

Scroll bar

Option 2: Calculate O'Neill (2021) SCSS (meas sulf comp)

```
ONeill_FixedSulf=ss.calculate_O2021_SCSS(df=df_out,
T_K=df_out['T_K'], P_kbar=df_out['P_kbar'],
Fe3Fet_Liq=df_out['Fe3Fet_Liq'],
Fe_FeNiCu_Sulf=0.65)
ONeill_FixedSulf.head()
```

Identical inputs to above, only difference is the function name!

Using inputted Fe_FeNiCu_Sulf ratio for calculations.

	SCSS2_ppm	LnS	Ln_a_FeO	Ln_a_FeS	DeltaG	LnCS2_calc	SiO2_Liq	TiO2_Liq	Al2O3_Liq	FeOt_Liq	MnO_Liq	MgO_Liq
0	1117.612680	7.018950	-2.405570	-0.495103	7.309272	-2.200789	49.9010	0.9981	14.9715	8.981890	0.0998	9.9763
1	1085.876342	6.990143	-2.401365	-0.495000	7.373234	-2.289456	49.9978	1.0081	15.1220	8.952251	0.1008	9.6064
2	1053.181390	6.959571	-2.397404	-0.494856	7.441489	-2.384467	50.0982	1.0185	15.2770	8.917591	0.1018	9.2279

Option 3: Calculate Li & Zhang (2022) SCSS (meas sulf comp)

```
LZ2022_FixedSulf=ss.calculate_LZ2022_SCSS(df=df_out,
T_K=df_out['T_K'], P_kbar=df_out['P_kbar'],
Fe3Fet_Liq=df_out['Fe3Fet_Liq'],
Fe_FeNiCu_Sulf=0.65)
LZ2022_FixedSulf.head()
```

Identical inputs to above, only difference is the function name!

Calculate trajectory if no sulfide (S behaving incompatibly)

```
FC=ss.crystallize_S_incomp(S_init=800, F_melt=df_out['Melt_%_magma']/100)
```

Plot modelled SCSS vs. incompatible FC trajectory with MI data

```
MI_data=pd.read_excel('MI_Data.xlsx') # Load MI data
fig, (ax1) = plt.subplots(1, 1, figsize=(4,3.5))
ax1.plot(df_out['MgO_Liq'], FC, 'k',
label='Incompatible behavior')
ax1.plot(Smythe_FixedSulf['MgO_Liq'],
Smythe_FixedSulf['SCSS2_ppm_ideal_ppm_Smythe2017'], '-r',
label='S2017 SCSS')
ax1.plot(LZ2022_FixedSulf['MgO_Liq'],
LZ2022_FixedSulf['SCSS_Tot'], '-c', label='LZ22 SCSS')
ax1.plot(ONeill_FixedSulf['MgO_Liq'],
ONeill_FixedSulf['SCSS2_ppm'], '-b', label='O2021 SCSS')
ax1.plot(MI_data['MgO_Liq'], MI_data['S_ppm'],
'k', mfc='yellow', label='MI')
ax1.set_ylabel('S (ppm)')
ax1.set_xlabel('MgO Liq (wt%)')
ax1.legend(fontsize=8, loc='lower right')
plt.xlim([4, 10])
plt.ylim([200, 1300])
```

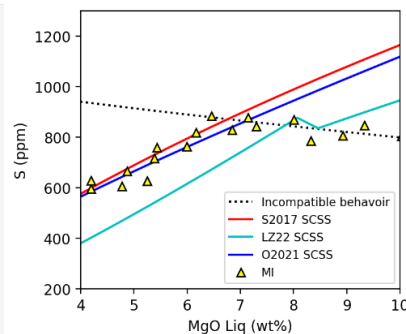


Figure 4: Annotated worked example showing how to calculate SCSS²⁻ for a Petrolog3 fractional crystallization path using a fixed Fe/(Fe+Ni+Cu) ratio in the sulfide. Hypothetical melt inclusion data is overlain. The data initially follows the incompatible fractional crystallization trend, followed by a prominent downturn, indicating the onset of sulfide saturation at ~ 6-7 wt% MgO.

289 3.2 Calculating Sulfide Compositions

While using a measured sulfide composition is the simplest and most reliable method to perform SCSS²⁻ calculations, direct measurements of sulfide compositions do not exist in many systems. PySulfSat allows users to calculate sulfide composition from Ni and Cu contents of the liquid using the approaches implemented in the supporting spreadsheets of O'Neill [2021] and Smythe et al. [2017]. The O'Neill [2021] method is the simplest, calculating the atomic Fe/(Fe+Ni+Cu) ratio using the following empirical expression:

$$\left(\frac{Fe}{Fe+Ni+Cu}\right)_{sulf} = \frac{1}{1 + 0.031 \frac{Ni_{Liq, ppm}}{FeO_{Liq, wt}} + 0.025 \frac{Cu_{Liq, ppm}}{FeO_{Liq, wt}}} \quad (1)$$

Where:

$$FeO_{Liq, wt} = FeO_{tLiq, wt} \times (1 - Fe^{3+}/Fe_T) \quad (2)$$

If the sulfide composition is not known, the spreadsheet of Smythe et al. [2017] has a sheet which will iteratively calculate the sulfide composition based on the partition coefficients of Cu and Ni in the sulfide from Kiseeva and Wood [2015]. These partition coefficients are sensitive to temperature, liquid FeO content, and the Ni and Cu content of the sulfide. Starting with a first estimate of the sulfide Ni and Cu content, the temperature, and the FeO content of the liquid, a partition coefficient can be calculated. Using this partition coefficient along with the initial estimate of the Ni and Cu content in the sulfide, the amount of Cu and Ni in a melt in equilibrium with this sulfide can be calculated. Smythe et al. [2017] define a residual between this calculated value and the measured Ni and Cu contents of the melt:

$$residual = (Ni_{Liq}^{Calc} - Ni_{Liq}^{Meas})^2 + (Cu_{Liq}^{Calc} - Cu_{Liq}^{Meas})^2 \quad (3)$$

290 The Excel solver function varies the Ni and Cu in the
 291 sulfide to obtain the values which best minimise this
 292 residual. Then, the equation of Kiseeva and Wood
 293 [2015] is used to calculate the Fe content of the sul-
 294 fide for these best fit sulfide Ni and Cu contents,
 295 and these 3 parameters are used to calculate the sul-
 296 fide Fe/(Fe+Ni+Cu) ratio. In PySulfSat, this conver-
 297 gence routine is performed using the scipy optimize
 298 minimize function (Virtanen et al. [2020]). In Ex-
 299 cel, for many compositions, the result obtained can
 300 depend slightly on the starting value of the Ni and
 301 Cu contents in the sulfide provided by the user. By
 302 default, the PySulfSat minimisation starts with ini-
 303 tial Ni and Cu contents of 5 wt%, but these param-
 304 eters can be overwritten using Cu_Sulf_init=10 and
 305 Ni_Sulf_init=5. These parameters are allowed to
 306 vary between 0-30 wt%. In general, we find our

python implementation of this solver method is stable and gives identical results to the Excel version for the same starting composition (and the vast majority of samples converge regardless of the starting Ni and Cu contents).

To perform SCSS calculations with modeled sulfide compositions, a string should be entered into the Fe_FeNiCu_Sulf argument. For example, to use the Smythe et al. [2017] SCSS²⁻ model with the O'Neill [2021] calculated sulfide composition, enter Fe_FeNiCu_sulf='Calc_O'Neill'. Users must also specify the Cu and Ni content in the liquid. In the example below, Ni_Liq (ppm) and Cu_Liq (ppm) are columns in the loaded dataframe df_out containing estimated Ni and Cu contents of the melt in ppm:

```
S17_SCSS_S17_Sulf=ss.calculate_S2017_SCSS(df=df_out,
Fe_FeNiCu_Sulf="Calc_O'Neill",
T_K=df_out['T_K'], P_kbar=df_out['P_kbar'],
Fe3Fet_Liq=df_out['Fe3Fet_Liq'],
Ni_Liq=df_out['Ni_Liq (ppm)'],
Cu_Liq=df_out['Cu_Liq (ppm)'])
```

Similarly, to use the O'Neill [2021] SCSS²⁻ model with the Smythe et al. [2017] calculated sulfide composition, specify Fe_FeNiCu_Sulf='Calc_Smythe':

```
021_SCSS_S17_Sulf=ss.calculate_02021_SCSS(df=df_out,
Fe_FeNiCu_Sulf="Calc_Smythe",
T_K=df_out['T_K'], P_kbar=df_out['P_kbar'],
Fe3Fet_Liq=df_out['Fe3Fet_Liq'],
Ni_Liq=df_out['Ni_Liq (ppm)'],
Cu_Liq=df_out['Cu_Liq (ppm)'])
```

3.3 H₂O-sensitivity

Unlike the SCSS²⁻ model of O'Neill [2021] which contain no term for H₂O, the SCSS²⁻ models of Fortin et al. [2015], and Smythe et al. [2017], Liu et al. [2021], Blanchard et al. [2021] and Li and Zhang [2022] are sensitive to the amount of H₂O in the liquid. By default, the SCSS²⁻ functions for each of these models (Fig. 2) use the H₂O content stored in the data loaded by the user in the column H2O_Liq. However, this can also be overwritten in the function itself, to allow investigation of the sensitivity of calculations to melt water content. For example, to perform all calculation at 3 wt% H₂O using the Fortin et al. [2015] model:

```
F2015_3H=ss.calculate_F2015_SCSS(df=df_out,
T_K=df_out['T_K'], P_kbar=df_out['P_kbar'],
H2O_Liq=3)
```

The argument H2O_Liq could also be set to a pandas series (e.g., any other column in the loaded data), which would allow calculations to

344 be performed using several different water con-
 345 tents (e.g., `df_out['Raman_H2O']` for Raman spec-
 346 troscopy measurements vs. `df_out['SIMS_H2O']`
 347 for SIMS measurements in the same samples).

348 3.4 Redox sensitivity

349 A number of SCSS models are also sensitive to the
 350 ratio of Fe^{3+} , because they contain a term for only
 351 Fe^{2+} species in the melt (see Fig. 2). The input ar-
 352 gument `Fe3Fet_Liq` should be supplied when us-
 353 ing these models. If no value is entered, calcu-
 354 lations are performed assuming $\text{Fe}^{3+}=0$. Alterna-
 355 tively, users can specify a single value in the func-
 356 tion (e.g., `Fe3Fet_Liq=0.15`), or refer to a column
 357 in the input dataframe. Another option is to use the
 358 Python package Thermobar (Wieser et al. [2022])
 359 to convert a $\log f\text{O}_2$ value or buffer position into a
 360 `Fe3Fet_Liq` ratio. For models which are not redox-
 361 sensitive (e.g., Blanchard et al. [2021], Liu et al.
 362 [2021]), entering a non-zero value for `Fe3Fet_Liq`
 363 will not affect the SCSS (except through secondary
 364 dependencies, e.g., if the model of Smythe et al.
 365 [2017] or O'Neill [2021] is used to calculate the sul-
 366 fide composition).

367 3.5 Calculating sulfide proportions

The difference between the fractional crystallization trajectory and the predicted SCSS²⁻ can be used to calculate the cumulative mass proportion of sulfide forming over the fractionation interval (after Kiseeva and Wood [2015]):

$$X_{\text{Sulf}} = \frac{S_{\text{init}} - F_{\text{melt}} * S_{\text{model}}}{S_{\text{sulf}}} \quad (4)$$

368 Where S_{init} is the initial S content at the start of the
 369 fractional crystallization sequence ($F_{\text{melt}}=1$), F_{melt} is
 370 the melt fraction remaining at each step, S_{model} is
 371 the modeled solubility of S in the melt, and S_{sulf}
 372 is the S content of the sulfide (all concentrations in
 373 ppm).

374 In PySulfSat, this is calculated as follows for the
 375 example shown in Fig. 4:

```
S_Frac=ss.calculate_mass_frac_sulf(
S_model=ONeill_FixedSulf['SCSS2_ppm'],
S_sulf=320000, S_init=800,
F_melt=df_out['Fraction_melt']/100)
```

376 This calculates the mass fraction of sulfide formed
 377 for a magma with 800 ppm S initially, a S content
 378 in the sulfide of 32 wt%, and a melt fraction from
 379 the Petrolog3 file (column heading `Fraction_melt`,
 380 obtained from the column `Melt_%_magma` in the
 381 Petrolog3 file by the PySulfSat import function).

382 4 SCAS⁶⁺ MODELS

383 In PySulfSat, SCAS⁶⁺ calculations are performed in
 384 a very similar way to SCSS²⁻ calculations. For ex-
 385 ample, to calculate SCAS⁶⁺ for the Petrolog3 model
 386 loaded in as `df_out` using the model of Chowdhury
 387 and Dasgupta [2019]:

```
CD19_SCAS=ss.calculate_CD19_SCAS(df=df_out,
T_K=df_out['T_K'])
```

388 The calculation could also be performed using
 389 the SCAS⁶⁺ model of Zajacz and Tsay [2019]:

```
ZT22_SCAS=ss.calculate_ZT2022_SCAS(df=df_out,
T_K=df_out['T_K'])
```

390 As for SCSS²⁻ models, these functions return the
 391 calculated SCAS⁶⁺, all intermediate calculations,
 392 and the originally-loaded compositions. The main
 393 simplification relative to SCSS models is the fact
 394 that none of the existing SCAS models have a term
 395 for the composition of the sulfate-bearing phase,
 396 pressure, or the $\text{Fe}^{3+}/\text{Fe}_T$ ratio (Fig. 2).

397 5 MAGMAS WITH A MIX OF S²⁻ AND S⁶⁺

398 Silicate melts undergo a relatively abrupt transi-
 399 tion in S speciation from sulfide (S^{2-}) to sulfate
 400 (S^{6+}) dominated with increasing oxygen fugacity
 401 (Fincham and Richardson [1954]; Jugo et al. [2010];
 402 Kleinsasser et al. [2022]; Wallace and Carmichael
 403 [1994], cyan line, Fig. 5b). In systems where both
 404 S^{2-} and S^{6+} are present, the calculated SCSS²⁻ will
 405 underestimate the total solubility of S, because this
 406 parameter only accounts for the solubility of S^{2-}
 407 species. Similarly, in systems dominated by S^{6+} with
 408 some S^{2-} , the total solubility of S will exceed the
 409 SCAS⁶⁺ (Jugo [2009]).

410 5.0.1 Demonstrating the importance of S²⁻ and 411 S⁶⁺ corrections

412 To demonstrate the importance of accounting for
 413 both S^{2-} and S^{6+} species when modeling total S sol-
 414 ubility, lets consider a melt with an SCSS²⁻ of 1000
 415 ppm, and an SCAS⁶⁺ of 5000 ppm. Equation 10 of
 416 Jugo et al. [2010] can be used to calculate the pro-
 417 portion of S^{6+}/S_T as a function of ΔQFM between
 418 -1 and +3:

$$\frac{\text{S}^{6+}}{\text{S}_T} = \frac{1}{1 + 10^{2.1 - 2\Delta\text{FMQ}}} \quad (5)$$

419 This equation can be implemented in PySulfSat
 420 for a single ΔQFM value as follows:

```
S6St_03=ss.calculate_S6St_Jugo2010_eq10(deltaQFM=0.3)
= 0.030653430031715508
```

421 To produce the cyan line on Fig. 5b, we input
 422 a linearly-spaced numpy array of 10,001 points be-
 423 tween ΔQFM=-1 and ΔQFM=3 generated using the
 424 np.linspace function, and calculate S⁶⁺/S_T for ev-
 425 ery value in this array (cyan line, Fig. 5b).

```
deltaQFM=np.linspace(-1, 3, 10001)
S6St=ss.calculate_S6St_Jugo2010_eq10(
    deltaQFM=deltaQFM)
```

426 At ΔQFM=-1 (point 1 on Fig. 5b), the melt is suf-
 427 ficiently reduced that only S²⁻ is dissolved in mean-
 428 ingful quantities (S⁶⁺/S_T=0.00008). Thus, the total
 429 solubility of sulfur is well approximated by the
 430 SCSS²⁻ (1000 ppm for this specific example, hori-
 431 zontal magenta line on Fig. 5a).

For a moderately oxidized melt at ΔQFM=1 (Point 2), S⁶⁺/S_T=0.442, so the presence of S⁶⁺ species substantially increases the total amount of S that is dissolved. Thus, the SCSS²⁻ must be corrected to obtain the SCSS_T using the equation of Jugo et al. [2010]:

$$SCSS_T = \frac{SCSS^{2-}}{1 - \frac{S^{6+}}{S_T}} \quad (6)$$

432 In PySulfSat this is implemented as follows:

```
S6=ss.calculate_S6St_Jugo2010_eq10(
    deltaQFM=1)
SCSS_Tot=ss.calculate_SCSS_Total(SCSS=1000,
    S6St_Liq=S6)
= 1794
```

433 The SCSS_T comprises with 1000 ppm of S²⁻, and
 434 794 ppm of S⁶⁺ (see red and grey lines on Fig. 5b).

435 At ΔQFM=1.39 (Point 3), S⁶⁺/S_T=0.827. Using
 436 eq6, the SCSS_T is 5786 ppm, with 1000 ppm of
 437 S²⁻, and 4786 ppm of S⁶⁺. However, if ΔQFM (and
 438 therefore S⁶⁺/S_T) increases slightly more, eq6 be-
 439 comes invalid, because the amount of predicted S⁶⁺
 440 exceeds the SCAS⁶⁺ (dashed magenta line, Fig. 5a).
 441 For example, at point 4 (ΔQFM=2), S⁶⁺/S_T=0.988.
 442 Equation 6 would predict that the SCSS_T is 80,433
 443 ppm, with 1000 ppm of S²⁻, and 79,433 ppm of S⁶⁺.
 444 However, this much S⁶⁺ cannot dissolve, because the
 445 SCAS⁶⁺ is only 5000 ppm.

Instead of correcting the SCSS for S⁶⁺, in more oxidising magmas, we can also correct the SCAS⁶⁺ for the presence of S²⁻:

$$SCAS_T = \frac{SCAS^{6+}}{1 - \frac{S^{2-}}{S_T}} \quad (7)$$

446 For example, at point 4:

```
SCAS_Tot=ss.calculate_SCAS_Total(SCAS=5000,
    S6St_Liq=0.988)
=5063
```

This total dissolved S comprises 5000 ppm of S⁶⁺ and 63 ppm of S²⁻. However, if this equation was applied to point 2, it would predict more dissolved S²⁻ than the SCSS. These worked examples demonstrates that at certain proportions of S⁶⁺ to S²⁻, Equations 7 and 6 are invalid to predict the total solubility of S. For the specific SCSS²⁻ and SCAS⁶⁺ values used in this example, ΔQFM= ~1.4 is the oxygen fugacity where the maximum amount of S dissolves in the system, because at this ΔQFM value, the ratio of S⁶⁺/S_T is such that the amount of S²⁻ dissolved is equal to the SCSS²⁻, and the amount of S⁶⁺ is equal to the SCAS⁶⁺ (yielding the maximum possible sum of these two values).

The total amount of dissolved S in ΔQFM space that does not violate the calculated SCSS²⁻ and SCAS⁶⁺ is defined by the section of the SCSS_T curve where S⁶⁺ does not exceed the SCAS⁶⁺ (magenta solid line, Fig. 5a), and the section of the SCAS_T curve where S²⁻ doesn't exceed the SCSS²⁻ (black solid line, Fig. 5a). The combined curve meeting these requirements is shown as a green line in Fig. 5b.

In PySulfSat, for any calculated SCSS²⁻ and SCAS⁶⁺ values, the total amount of S can be calculated using the function calculate_S_Total_SCSS_SCAS. This can be used to produce plots of changing S speciation with fO₂ (e.g., Fig. 5).

For example, using 11 equally spaced ΔQFM values between -1 and 3 (-1, -0.6, -0.2...), we can calculate the total solubility of S using the model of Jugo et al. [2010], for a fixed SCSS²⁻ (1000 ppm) and SCAS⁶⁺ value (5000 ppm):

```
deltaQFM_lin=np.linspace(-1, 3, 10)
df_S_Jugo=ss.calculate_S_Total_SCSS_SCAS(
    deltaQFM=deltaQFM_lin,
    SCSS=1000, SCAS=5000, model='Jugo')
```

This function returns a pandas dataframe:

	Total_S_ppm	S2_Tot_ppm	S6_Tot_ppm	deltaQFM	S6St_Liq	SCSS_2_ppm	SCAS_6_ppm
0	1000.079433	1000.000000	0.079433	-1.000000	0.000079	1000	5000
1	1000.615020	1000.000000	0.615020	-0.555556	0.000615	1000	5000
2	1004.761873	1000.000000	4.761873	-0.111111	0.004739	1000	5000
3	1036.869451	1000.000000	36.869451	0.333333	0.035558	1000	5000
4	1285.466766	1000.000000	285.466766	0.777778	0.222072	1000	5000

The column Total_S_ppm shows the total amount of S dissolved in ppm, with an amount of S²⁻ indicated by the column S2_Tot_ppm and S⁶⁺ by the column S6_Tot_ppm. The input SCSS and SCAS are also shown in columns SCSS_2_ppm and SCAS_6_ppm; the values in the columns S2_Tot_ppm and S6_Tot_ppm will always be less than or equal to these values.

In addition to the Jugo et al. [2010] model which calculates S⁶⁺/S_T in terms of ΔQFM, calculations can also be performed in PySulfSat using the Nash et al. [2019] model, which parameterizes S⁶⁺/S_T in

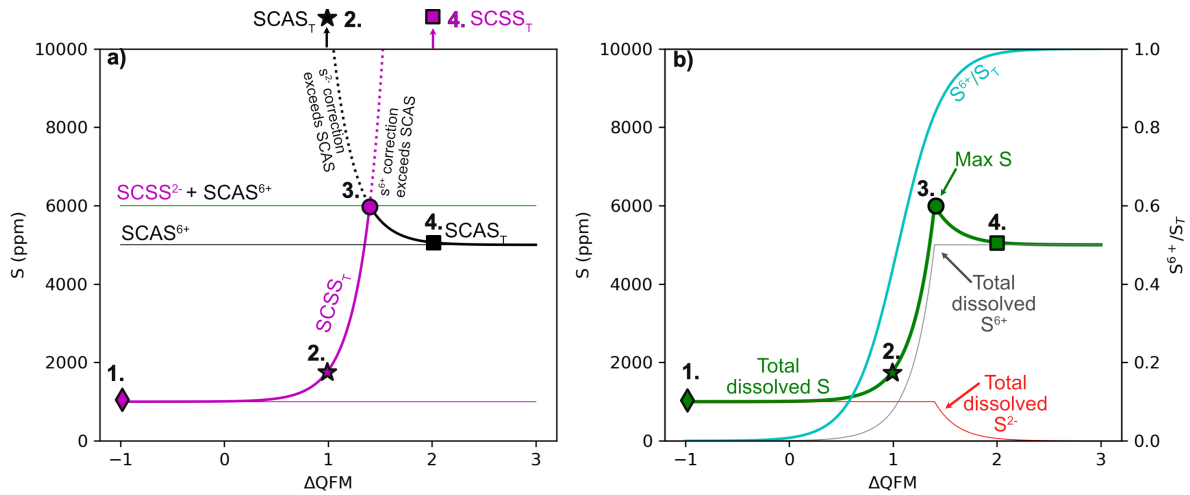


Figure 5: Calculating the total amount of dissolved S by applying corrections for the presence of both S species using the model of Jugo et al. [2010] in the function `calculate_S_Total_SCSS_SCAS`. These graphs were drawn for $SCSS^{2-}=1000$ ppm and $SCAS^{6+}=5000$ ppm, although these numbers could be calculated using any SCSS and SCAS model in PySulfSat.

terms of the ratio of Fe^{3+} to Fe^{2+} and temperature (in Kelvin):

$$\log\left(\frac{S^{6+}}{S^{2-}}\right) = 8\log\left(\frac{Fe^{3+}}{Fe^{2+}}\right) + \frac{8.7436 \times 10^6}{T^2} - \frac{27703}{T} + 20.273 \quad (8)$$

To calculate S^{6+}/S_T using this model, the temperature in Kelvin and the ratio of Fe^{3+}/Fe_T must be input:

```
Calc_Nash_S6=ss.calculate_S6St_Nash2019(
T_K=df_out['T_K'], Fe3Fet_Liq=df_out['Fe3Fet_Liq'])
```

When calculating the Total S content, specify `model='Nash'` rather than `model='Jugo'` in the function `calculate_S_Total_SCSS_SCAS`:

```
deltaQFM_lin=np.linspace(-1, 3, 11)
df_S_Nash=ss.calculate_S_Total_SCSS_SCAS(
deltaQFM=deltaQFM_lin,
SCSS=1000, SCAS=5000,
model='Nash', T_K=df_out['T_K'],
Fe3Fet_Liq=df_out['Fe3Fet_Liq'])
```

Kleinsasser et al. [2022] note that the transition predicted by models primarily calibrated on mafic melts (e.g., Nash et al. [2019]; Jugo et al. [2010]) is not a good match for dacitic melt compositions, where the transition occurs at higher fO_2 values ($\Delta QFM=+1.81 \pm 0.56$). They provide two expressions for correcting the $SCSS^{2-}$ and $SCAS^{6+}$:

$$\begin{aligned} SCSS_T^{dacitic} &= SCSS^{2-} * (1 - 10^{2\Delta QFM - 3.05}) \\ SCAS_T^{dacitic} &= SCAS^{6+} * (1 - e^{1.26 - 2\Delta QFM}) \end{aligned} \quad (9)$$

This parameterization can also be used in PySulfSat, by specifying `model='Kleinsasser'`:

```
deltaQFM_lin=np.linspace(-1, 3, 11)
df_S_Klein=ss.calculate_S_Total_SCSS_SCAS(
deltaQFM=deltaQFM_lin,
SCSS=1000, SCAS=5000,
model='Kleinsasser')
```

5.0.2 Calculating S^{6+}/S_T from the Sulfate and Sulfide capacity

In addition to the methods described above where the proportion of S species is estimated from oxygen fugacity or Fe^{3+}/Fe_T , the ratio of S^{6+}/S_T can also be calculated using the method of O'Neill and Mavrogenes [2022]. This approach calculates the sulfide capacity ($C_{S^{2-}}$) using the parameterization of O'Neill [2021], and the sulfate capacity ($C_{S^{6+}}$) using O'Neill and Mavrogenes [2022]. The equilibrium constant for the gas-phase equilibrium, $\ln K$, is then calculated using T in Kelvin:

$$\ln(K) = -55921/T + 25.07 - 0.6465 * \ln(T) \quad (10)$$

These values are then used to calculate S^{6+}/S^{2-} , which can be easily converted into a S^{6+}/S_T ratio:

$$\ln\left(\frac{S^{6+}}{S^{2-}}\right) = \ln(C_{S^{6+}}) - \ln(K) - \ln(C_{S^{2-}}) + 2\ln(10) * \log fO_2 \quad (11)$$

And:

$$\frac{S^{6+}}{S_T} = 1 - \frac{1}{1 + e^{\ln\left(\frac{S^{6+}}{S^{2-}}\right)}} \quad (12)$$

Their supporting spreadsheet also provides an option to input Fe^{3+}/Fe_T ratio instead of a value for $\log fO_2$. The spreadsheet uses this ratio to calculate ΔQFM using an adapted version of Eq9a of O'Neill

et al. [2018] (missing the term for P₂O₅, as this oxide isn't included in their capacity models):

$$\Delta QFM = 4 \left(\log \left(\frac{Fe^{3+}}{Fe_T} \right) + 1.36 - 2X_{Na} - 3.7X_K - 2.4X_{Ca} \right) \quad (13)$$

Where X_{Na}, X_K and X_{Ca} are the cation fractions of Na, K and Ca in the melt. This ΔQFM value is then converted into logfO₂ using Eq8 of O'Neill et al. [2018] based on O'Neill [1987] to input into Eq12:

$$\log_{10} fO_2 = \Delta QFM - 25050/T + 8.58 \quad (14)$$

Where T is in Kelvin.

These equations are all implemented in PySulfSat through the function calculate_OM2022_S6St. For example, to perform calculations using a known logfO₂ value:

Alternatively, users can enter a

```
Calc_OM2022=ss.calculate_OM2022_S6St(df=df_out,
T_K=Liqs['T_K'], logfo2=Liqs['logfo2'])
```

Alternatively, if the Fe³⁺/Fe_T ratio is stored in a column in the input dataframe:

```
Calc_OM2022=ss.calculate_OM2022_S6St(df=df_out,
T_K=Liqs['T_K'], Fe3Fet_Liq=Liqs['Fe3Fet_Liq'])
```

Which returns a pandas dataframe:

	S6St_Liq	LnCS2_calc	LnKSO2S2	LnS6S2	deltaQFM_calc	Sample ID
0	0.009061	-2.252326	-18.676809	-4.694696	0.385382	VG175
1	0.018402	-2.187329	-18.757549	-3.976697	0.549923	180
2	0.016171	-2.276202	-18.567275	-4.108246	0.468580	183
3	0.013897	-2.376010	-18.501180	-4.262089	0.417146	186
4	0.051541	-2.345865	-18.557150	-2.912471	0.721690	187

Boulliung and Wood [2022] also publish an equation to calculate log C_{S6+}. While related to the ln C_{S6+} value of O'Neill and Mavrogenes [2022], this is not simply a log-ln conversion. Boulliung and Wood [2022] express their S content in wt percent, rather than ppm, and their equilibrium constant refers to a different Equation. These values can be converted from one form to another (see ReadTheDocs for a derivation). In PySulfSat, the function calculate_BW2022_CS6 returns a dataframe for columns named 'LogCS6_calc_BW22_format' which uses the Boulliung and Wood [2022] format, and 'LnCS6_calc_OM22_format' which uses the format of O'Neill and Mavrogenes [2022]. This allows direct comparison between models. We also include the function calculate_BW2022_OM2022_S6St to calculate S⁶⁺/S_T using C_{S6+} from Boulliung and Wood [2022] and C_{S2-} from O'Neill [2021].

5.0.3 Calculations for natural samples

When calculating the total solubility of S in a natural system with a non negligible proportion of both S species, using the function calculate_S_Total_SCSS_SCAS ensures that the correction has not exceeded the solubility of either species, unlike functions correcting the SCSS for S⁶⁺ using calculate_SCSS_Total, or SCAS for S²⁻ using calculate_SCAS_Total.

When comparing measured S contents to total S solubility obtained from SCSS and SCAS models, it is most reliable to use measured S⁶⁺/S_T ratios (e.g., using XANES, Lerner et al. [2021]). In this ideal scenario, users can enter the measured ratio directly in the calculate_S_Total_SCSS_SCAS function. For example, after calculating the SCSS using Smythe et al. [2017] (saved in df=S2017) and the SCAS using Zajacz and Tsay [2019] (saved in df=Z2019), the total amount of dissolved S can be calculated using a fixed S⁶⁺/S_T ratio of 0.2:

```
Tot_S_S17_Z19=ss.calculate_S_Total_SCSS_SCAS(
SCSS=S2017['SCSS_ideal_ppm_Smythe2017'],
SCAS=Z2019['SCAS6_ppm'],
S6St_Liq=0.2)
```

Alternatively, it is more common that Fe³⁺/Fe_T has been constrained using XANES. Using the Nash et al. [2019] correction, this Fe³⁺/Fe_T ratio can be entered directly to calculate the S⁶⁺/S_T ratio, and thus the maximum amount of S that can dissolve:

```
Tot_S_S17_Z19_Nash=ss.calculate_S_Total_SCSS_SCAS(
SCSS=S2017['SCSS_ideal_ppm_Smythe2017'],
SCAS=Z2019['SCAS6_ppm'],
Fe3Fet_Liq=0.15, model='Nash')
```

For consistency, in this example, the S2017 dataframe should also have been calculated using the same input value for Fe3Fet_Liq=0.15.

To use the Jugo et al. [2010] correction, the redox state of the magma must be calculated relative to the QFM buffer position of Frost [1991] (see Section 5.1. If Fe³⁺/Fe_T is known, this can be converted into a log fO₂ value using Kress and Carmichael [1988] using the Python package Thermobar (Wieser et al. [2022]). Once a log fO₂ value is calculated, Thermobar can then be used to calculate the offset from the QFM buffer position (i.e. ΔQFM). Alternatively, this value may be known independently without having to do a conversion based on Fe³⁺/Fe_T first. For example, the Petrolog3 output in figure 4 has a column for the log of the fO₂ value, the temperature and the pressure.

```
!pip install Thermobar
import Thermobar as pt
Buffer_calc=pt.convert_fo2_to_buffer(
fo2=10**df_out['Lg(fO2)'],
T_K=df_out['T_K'], P_kbar=df_out['P_kbar'])
```

	deltaNNO_Frost1991	deltaQFM_Frost1991	QFM_equation_Choice	T_K	P_kbar	fo2	Cut off T (K)
0	-0.777890	-0.085829	High T	1526.431	1	1.905461e-08	871.15
1	-0.781999	-0.089502	High T	1516.580	1	1.479108e-08	871.15
2	-0.779077	-0.086116	High T	1506.214	1	1.148154e-08	871.15
3	-0.770841	-0.077393	High T	1495.511	1	8.912509e-09	871.15
4	-0.774373	-0.080406	High T	1484.230	1	6.606934e-09	871.15

The different buffers stored in the Buffer_calc dataframe can then be input into the PySulfSat function:

```
ss.calculate_S_Total_SCSS_SCAS(
  deltaQFM=Buffer_calc['deltaQFM_Frost1991'],
  SCSS=S2017['SCSS_ideal_ppm_Smythe2017'],
  SCAS=Z2019['SCAS6_ppm'],
  T_K=df_out['T_K'],
  model='Jugo')
```

Alternatively, if you have an estimate of fO_2 you can use the O'Neill and Mavrogenes [2022] method:

```
ss.calculate_S_Total_SCSS_SCAS(
  logfo2=df_out['Lg(fo2)'],
  SCSS=S2017['SCSS_ideal_ppm_Smythe2017'],
  SCAS=Z2019['SCAS6_ppm'],
  T_K=df_out['T_K'],
  model='OM2022')
```

This function can also take Fe^{3+}/Fe_T as input, although our code (and the published spreadsheet) convert this into a $\log(fO_2)$ value using Eq 13.

5.1 Different Buffer Positions and Melt Redox Models

It is important to recognize the uncertainty introduced into calculations of S^{6+} proportions as a result of different definitions of buffer positions, melt redox models, and XANES data processing strategies. For example, the ΔQFM values for the Jugo et al. [2010] S^{6+} correction should be relative to the QFM buffer position of Frost [1991]. Petrolog3 uses the expression of Myers and Eugster [1983] for its QFM buffer. AlphaMELTS (including MELTS for MATLAB and Python, Antoshechkina and Ghiorso [2018]) and MELTS for Excel (Gualda and Ghiorso [2015]) also use Myers and Eugster [1983], with an additional pressure correction from Frost [1991]. Expressing all these different QFM buffer positions in terms of $\log(fO_2)$ values at QFM yields the following equations:

$$\log fO_2 \text{ at QFM (Frost, 1991)} = \frac{-25,096.3}{T} + 8.735 + 0.11 \frac{P-1}{T} \quad (15)$$

$$\log fO_2 \text{ at QFM (O'Neill et al. 2018)} = \frac{-25,050}{T} + 8.58 \quad (16)$$

$$\log fO_2 \text{ at QFM (Petrolog3)} = \frac{-24,442}{T} + 8.29 \quad (17)$$

$$\log fO_2 \text{ at QFM, MELTS} = \frac{-24,442}{T} + 8.29 + 0.11 * \frac{(P-1)}{T} \quad (18)$$

Where P is in bars and T is in Kelvin. If users have a ΔQFM value relative to a buffer which is not

Frost [1991], they need to convert that into a value relative to the Frost [1991] prior to using Jugo et al. [2010]. To demonstrate the importance of performing these conversions, let's consider a melt at 1050° C and 200 MPa. Say a user has obtained a buffer position of $\Delta QFM+1$ relative to Eq 16. If this ΔQFM value was entered directly into Jugo et al. [2010], it would yield 45% S^{6+} . However, this buffer position should first be used to calculate the $\log(fO_2)$ value (-9.35), to then calculate the ΔQFM relative to Frost [1991] ($\Delta QFM=0.71$). This yields only 18% S^{6+} . This shows the importance of maintaining consistency with the buffer position used to calibrate Jugo et al. [2010].

There are a variety of methods to convert $\log(fO_2)$ values into Fe^{3+}/Fe_T ratios (see Putirka [2016]), which can introduce uncertainty when using the Nash et al. [2019] method, or when inputting ratios directly into the O'Neill and Mavrogenes [2022] method. For example, Petrolog3 allows users to choose between the models of Borisov and Shapkin [1990]; Kilinc et al. [1983]; Kress and Carmichael [1988]; Sack et al. [1981]. For the default Petrolog3 composition at $\Delta QFM=0$, atmospheric pressure and the liquidus position, these 4 models return Fe^{3+} proportions between 10 and 14%, which corresponds to S^{6+} proportions using Nash et al. [2019] of 1.2-24%. Of course, offsets between the selected definition of the QFM buffer (O'Neill-Petrolog3-Frost) will also affect the Fe^{3+} proportions calculated by different melt redox models (through influencing the $\log(fO_2)$ value).

The O'Neill and Mavrogenes [2022] method for calculating S^{6+} proportions is parameterized directly in terms of $\log(fO_2)$, so when pairing this model with various petrology modeling software, the easiest way to avoid mixing and matching buffer definitions/melt redox models is to directly input this parameter. If Fe^{3+}/Fe_T is entered, this is converted to $\log(fO_2)$ using O'Neill et al. [2018] Eq 8 and 9b (Equation 13-14 in this paper). This will return a different $\log(fO_2)$ to that outputted directly by MELTS/Petrolog3 (which use models other than O'Neill et al. [2018] to convert $\log(fO_2)$ to Fe^{3+}/Fe_T). When Fe^{3+}/Fe_T is measured directly by XANES, it is worth considering additional compilations resulting from different calibration strategies. For example, O'Neill and Mavrogenes [2022] make sure to correct the Fe XANES measurements of Brounce et al. [2017] and Muth and Wallace [2021] using the method of Berry et al. [2018] prior to performing calculations of S^{6+} proportions. However, we find that the S XANES measurements of Muth and Wallace [2021] are best matched by the O'Neill and Mavrogenes [2022] if measured Fe^{3+}/Fe_T ratios are input, rather than ratios corrected using Berry et al. [2018]. More comparisons are clearly required to see if this is a one-off occurrence. In many in-

stances, offsets between different Fe^{3+}/Fe_T XANES reduction methods, and Fe^{3+}/Fe_T -log(fO_2) conversion strategies should perhaps be considered as true error on these methods, given the lack of community consensus (Anenburg and O’Neill [2019]).

6 MONTE CARLO ERROR PROPAGATION

In addition to simplifying calculations and aiding model comparisons, PySulfSat also allows users to propagate uncertainty in input parameters for all calculation types using Monte Carlo methods. There are two main workflows that can be used. First, if errors are known for every input variable, users should load in two dataframes. The first dataframe (df1) should contain the preferred value for each input parameter (e.g., columns MgO_Liq, FeOt_Liq, H2O_Liq). The second dataframe (df2) should have exactly the same column headings with the addition of the suffix _Err. These columns can contain absolute or percentage errors. Additional columns (e.g. temperatures calculated using Thermobar, Wieser et al. [2022]) can be appended onto df1 in the Jupyter Notebook itself, along with an appropriate error in df2. The function add_noise_2_dataframes can then be used to duplicate each input row in the input dataframe df_values N_dups times, adding noise based on the value in the dataframe with errors (df_err). For example, to add normally distributed errors using absolute 1σ values from df2, and create 5000 duplicates for each sample:

```
df_noisy=ss.add_noise_2_dataframes(
df_values=df1, df_err=df2,
error_type="Abs", error_dist="normal",
N_dups=5000)
```

This new dataframe is then entered into any of the functions.

In Fig. 6 we use the add_noise_2_dataframes function to generate 5000 synthetic compositions for each melt inclusion, with errors from quoted 1σ values for each variable from Muth and Wallace [2021]. These synthetic compositions were then input into the various functions to calculate S^{6+}/S_T ratios. Finally, the function av_noise_samples_series is used to calculate statistics for each melt inclusion. Users should input a pandas.Series containing the variable of interest into this function as the argument var (in this case, the calculated S^{6+}/S_T ratio stored in the dataframe O'Neill_S6ST), and a second pandas.Series with the sample names to average over (as sampleID).

```
Stats_S6=pt.av_noise_samples_series(
calc=ONeill_S6ST['S6St_Liq'],
sampleID=df_noisy['Sample_ID_Liq'])
Stats_S6.head()
```

For example, the first row in the output averages all 5000 simulations for rows with the sample name BBL-5-32.

	Sample	# averaged	Mean_calc	Median_calc	St_dev_calc	Max_calc	Min_calc
0	BBL-5-32	5000	0.031770	0.015473	0.046489	0.642037	9.926852e-06
1	BBL-5-33	5000	0.449445	0.443940	0.212362	0.949757	1.100763e-02
2	BBL-5-34	5000	0.143123	0.099256	0.134041	0.813120	4.726367e-04
3	BBL-5-43	5000	0.131442	0.086405	0.129857	0.839532	1.181191e-04
4	BBL-5-44	5000	0.018558	0.007207	0.031935	0.403228	7.200104e-08

This function calculates the mean, median, max, min and standard deviation of all 5000 simulations for each melt inclusion (which are used to plot symbols and error bars on Fig. 6f-h). Simulations can be conducted for any of the calculations available in PySulfSat (e.g. SCSS, SCAS, K_D etc.).

A second set of functions can be useful when you want to explore noise in a smaller number of input variables (e.g. just T, T and H₂O), or where some errors are absolute, some are percente, some are normal and some are uniformly-distributed. The function duplicate_dataframe takes a dataframe and duplicates the values in each row N_dup times (row1-row2-row3 goes to row1-row1-row1..., row2-row2-row2....):

```
Dupdf=ss.duplicate_dataframe(df=df1, N_dup=5000)
```

Then the function add_noise_series can be used to create a pandas.Series of noise for one specific variable with the same length as this larger dataframe. For example, EDS measurements in a suite of lavas may reveal the sulfide composition for sample 1 is $Fe/(Fe+Ni+Cu)=0.65$, and sample 1 is 0.8, with an error of ± 0.05 (stored in the column df1['Sulf_X']). Here, we add normally distributed noise, with 5000 duplicates for each input (to match the dataframe above).

```
sulf_comp_err=ss.add_noise_series(var=df1['Sulf_X'],
error_var=0.05, error_type="Abs",
error_dist="normal", N_dup=5000)
```

For example, the first 5000 rows in this new pandas.Series may read 0.64, 0.65, 0.67, 0.65...N₅₀₀₀, and the next 5000 rows may read 0.81, 0.8, 0.79, 0.82...N₅₀₀₀. The total length is the number of rows input multiplied by the number of duplicates, which is the same as the duplicated dataframe. Thus, this new pandas.Series can be appended onto this dataframe as a column:

```
Dupdf['Sulf_MC']=sulf_comp_err
```

As many 'noisy' columns can be added as the user wishes, with different error types and distributions. This dataframe where some columns have noise added and some do not can then be input into any of the PySulfSat functions.

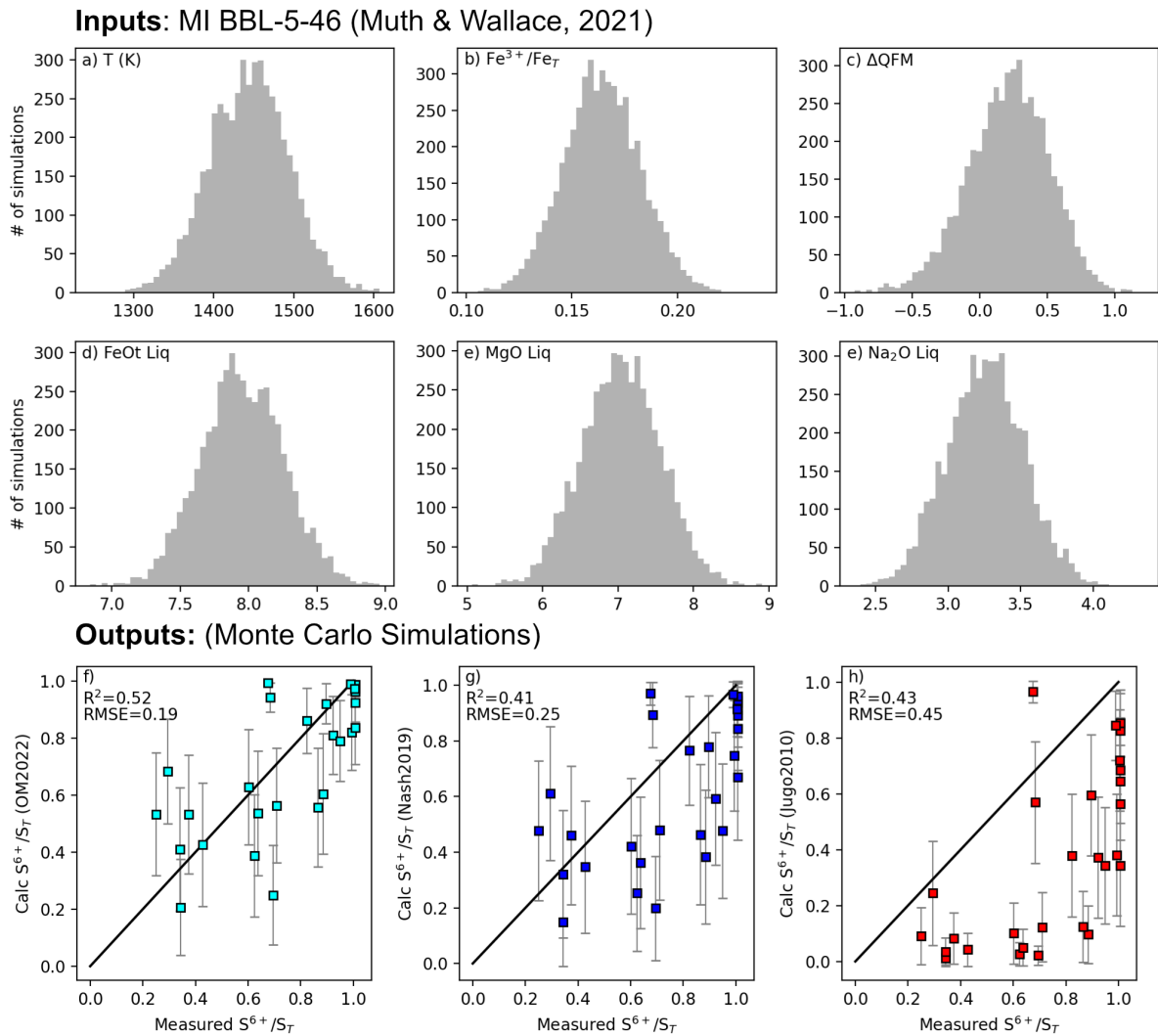


Figure 6: Using Monte Carlo simulations to investigate errors associated with different methods of calculating S^{6+}/S_T ratios. For each melt inclusion, 5000 synthetic compositions were generated using quoted 1σ values from Muth and Wallace [2021] (distributions for MI BBL-5-46 are shown in a-e). In f-h), we show 1σ errors for each method of calculating S^{6+}/S_T . A detailed worked example showing how to produce this figure can be found at ReadTheDocs.

7 INTEGRATION WITH MELTS

While PySulfSat can load the results from a MELTS calculation as a .tbl file, recent advances in the MELTS computing infrastructure means that MELTS fractional crystallization calculations can be performed directly in Python in the same Jupyter Notebook as PySulfSat calculations. There are currently two options for performing MELTS calculations in Python; Thermoengine (Johnson et al. [2022]) and alphaMELTS for Python (Antoshechkina and Ghiorso [2018]). We make use of the PyMELTScalc python package Gleeson et al. [2023]), which provides neatly wrapped functions for fractional crystallization using alphaMELTS for Python, and returns output structures consistent with the required inputs for PySulfSat.

After installing PyMELTScalc (see example on ReadTheDocs), this package must be imported into the notebook:

```
import pyMELTScalc as M
```

After loading data using the `ss.import_data` function as `df_out`, a specific melt composition can be selected as a starting composition (here, we select the first row):

```
sample=df_out.iloc[0]
```

Then, a MELTS fractional crystallization model can be initiated at a single pressure using the `multi_path` function:

```
MELTS_FC=M.multi_path(
    model="MELTSv1.0.2",
    comp = sample,
    P_bar = 1000,
    find_liquidus = True,
    T_end_C = 750,
    dt_C = 5,
    Fe3Fet_Liq=0.1,
    Frac_solid = True,
    Frac_fluid = True)
```

This runs a fractional crystallization model at 1000 bars (`P_bar`), starting at the wet liquidus (`find_liquidus=True`), and runs until 700° C (`T_end_C`). If the MELTS calculation doesn't converge after 100 quadratic minimisation attempts, the simulation may end at a higher temperature. The temperature step is 5 °C (`dt_C`), the initial `Fe3Fet_Liq` ratio is set at 0.1, and both fluids and solids are fractionated.

This `multi_path` function outputs a dictionary containing a series of dataframes. There is a dataframe for each phase, but most relevant for this work is the dataframe named 'All'. This contains all the relevant outputs stitched together, and can be obtained from the overall output as follows:

```
MELTS=MELTS_FC['All']
```

This dataframe named MELTS contains system properties (T, P, enthalpy, entropy, volume) and the composition of each phase with the phase name as an underscore (e.g. `SiO2_Liq`, `SiO2_Plag` etc.). It can be fed directly into the PySulfSat code. For example, lets use the model of Li and Zhang [2022] for a specified sulfide composition:

```
LiZhang22=ss.calculate_LZ2022_SCSS(df=MELTS,
    T_K=MELTS['T_C']+273.15,
    P_kbar=MELTS['P_bar']/1000,
    H2O_Liq=MELTS['H2O_Liq'],
    Fe_FeNiCu_Sulf=0.6,
    Fe3Fet_Liq=MELTS['Fe3Fet_Liq'])
```

PyMELTScalc can also be used to investigate a wide range of different fractional crystallization paths using parallel processing for computational efficiency, with hundreds to thousands of different fractional paths initiated with a single function call. For example, coupling of PyMELTScalc and PySulfSat would allow users to investigate S behavior during fractional crystallization for a single melt or range of melt compositions over a wide variety of different starting pressures, oxygen fugacities, and melt water contents. Fig. 7 shows the SCSS²⁻ calculated for fractional crystallization models run at 4 different pressures from a single call to the PyMELTScalc `multi_path` function. PyMELTScalc can run calculations at a redox buffer or unbuffered, so calculations can be implemented with the various options for the treatment of S⁶⁺ to investigate changes in S speciation during fractional crystallization.

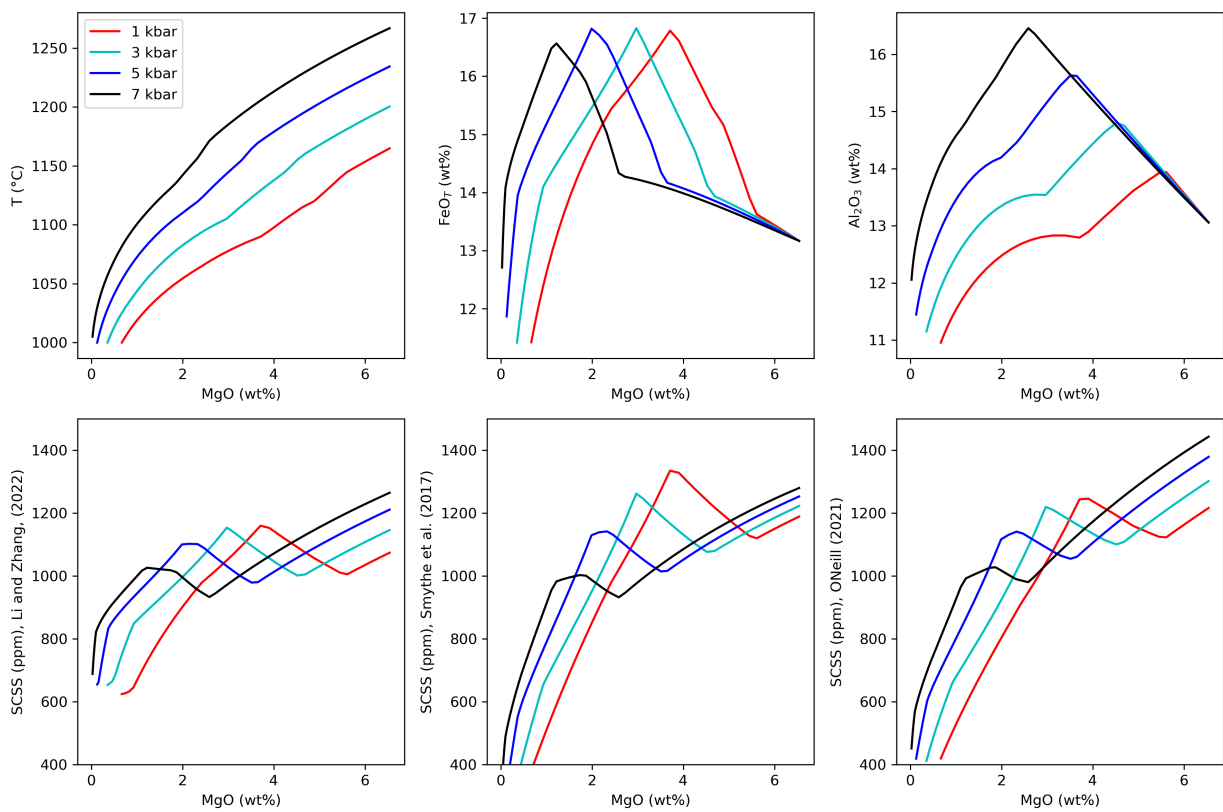


Figure 7: Integrating PyMELTScalc and PySulfSat to model the SCSS for a fractional crystallization at 4 different pressures. Worked examples showing how to produce this and other similar plots are available on the ReadTheDocs page.

8 MANTLE MELTING CALCULATIONS

Modeling the concentrations of S, Cu and other chalcophile elements during mantle melting is complicated by the fact that these elements are held in silicate minerals and mantle sulfides. Because mantle melts contain higher S contents than the mantle residue, the mantle becomes more and more depleted in sulfide during progressive melting until the sulfide phase is eventually exhausted (Wieser et al. [2020], Ding and Dasgupta [2018], Lee et al. [2012]). Exhaustion of sulfide in the mantle residue drives a large change in the bulk partition coefficient of chalcophile elements during the melting interval.

Lee et al. [2012] provide an Excel spreadsheet for calculating the concentration of Cu during near-fractional melting. This model removes small batch melts, updating the composition of the remaining mantle residue before the next melting step proceeds. The Equation for batch melting is as follows:

$$\frac{C_{melt}}{C_{source}} = \frac{1}{D_0 + F(1 - P)} \quad (19)$$

Where C_{melt} is the concentration in the melt, C_{source} is the concentration in the mantle source, D_0 is the bulk partition coefficient (sulfide+silicate) at the start of that melting step, F is the degree of melt produced in that melt step, and P is the bulk partition coefficient weighted for the proportion that each component enters the melt. For simplicity, Lee et al. [2012] assume that $D_0=P$ (e.g. sulfide and silicate minerals melt at the same rate). Wieser et al. [2020] update this model to account for non-modal melting behavior, because the sulfide preferentially melts, so contributes more to the partition coefficient of highly chalcophile elements such as Cu than the silicates. It should be noted that at a small enough step size (i.e. small enough ΔF), the results from these two approaches converge. However, using the limited number of columns supplied in the spreadsheet of Lee et al. [2012], the divergence can be several 10s of ppm at a given extent of melting (F).

We implement the non-modal melting version of Wieser et al. [2020] in PySulfSat with the function `Lee_Wieser_sulfide_melting`. This function can be used to model the concentration of any element during near fractional batch melting, and allows the contrasting behavior of chalcophile and lithophile elements to be modeled (e.g., Ba vs. Cu, Wieser et al. [2020]). The user must supply a dataframe with partition coefficients for silicate and sulfide phases, and the mass proportion of each phase. In Fig. 8a-b, we calculate the concentration of Cu and Ba in aggregated melts for different melt extents. First, we specify the silicate modes:

```
Modes=pd.DataFrame(data={'o1': 0.6, 'opx': 0.2,
                          'cpx': 0.18, 'sp': 0.02, 'gt': 0}, index=[0])
```

And the partition coefficients:

```
KDs_Cu=pd.DataFrame(data={'element': 'Cu',
                          'o1': 0.048, 'opx': 0.034,
                          'cpx': 0.043, 'sp': 0.223,
                          'gt': 0, 'sulf': 800}, index=[0])
```

```
KDs_Ba=pd.DataFrame(data={'element': 'Ba',
                          'o1': 0.000005, 'opx': 0.000006,
                          'cpx': 0.0004, 'sp': 0.223,
                          'gt': 0.00007, 'sulf': 0 }, index=[0])
```

For simplicity in this example, we assume that the silicate modes stay fixed throughout the melting interval. This assumption makes very little difference for Cu, as the partition coefficient is substantially higher for sulfides than any silicate phases. Even for Ba, this is a reasonable 1st order assumption because it is extremely incompatible in all high abundance silicate phases. The other required inputs are:

1. The number of iterative steps (N=3000)
2. The S content of the mantle source in ppm (S_Mantle=200)
3. The concentration of S in mantle sulfides in ppm (S_Sulf=360000)
4. The initial concentration of the element of interest in the mantle prior to melting in ppm (elem_Per=30)
5. The S^{2-} concentration of the melt in ppm (S_Melt_SCSS_2=1000).
6. The proportion of S^{6+} (here Prop_S6=0), which will be used alongside the S^{2-} concentration to calculate the total amount of S in the melt using Eq 6:

These inputs are then used as follows for Cu:

```
df_Cu_200S=ss.Lee_Wieser_sulfide_melting(N=3000,
Modes=Modes, KDs=KDs_Cu, S_Mantle=200,
S_Sulf=360000, S_Melt_SCSS_2_ppm=1000,
elem_Per=30, Prop_S6=0)
```

and Ba:

```
df_Ba_200S=ss.Lee_Wieser_sulfide_melting(N=3000,
Modes=Modes, KDs=KDs_Ba, S_Mantle=200,
S_Sulf=360000, S_Melt_SCSS_2_ppm=1000,
elem_Per=6.85, Prop_S6=0)
```

These calculations were run at S_Mantle contents of 100 ppm, 200 ppm and 300 ppm to produce Fig. 8a-b).

In addition to the ease of the above calculations vs. existing tools, the other substantial advantage of PySulfSat is that it allows integration of melting models with models for partition coefficients in sulfides, and models of the SCSS within a single

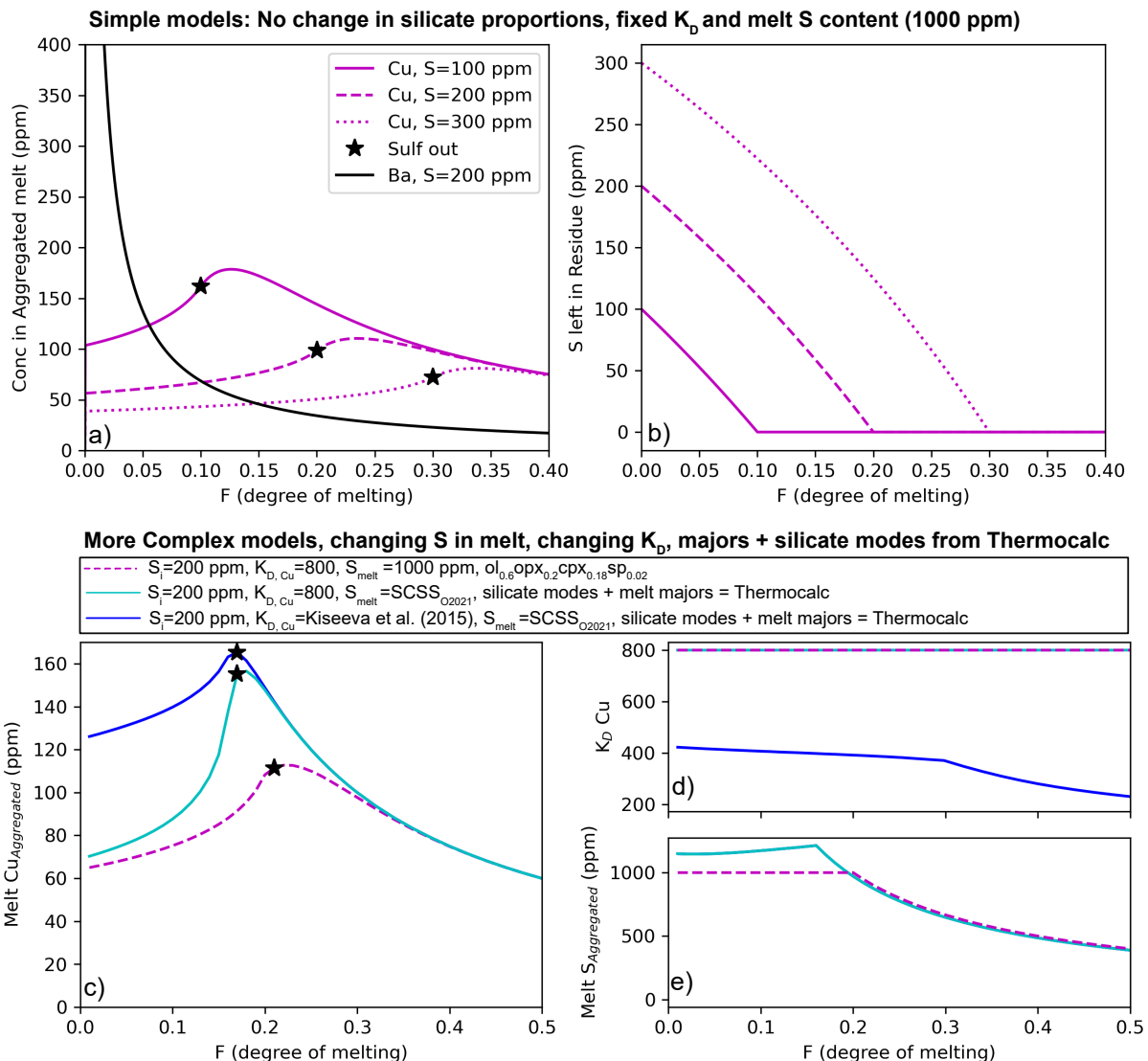


Figure 8: Modeling chalcophile elements during mantle melting. a-b) Simple models following [Lee et al. \[2012\]](#) and [Wieser et al. \[2020\]](#) where the K_D in the sulfide, the modal proportion of silicate minerals and S in the melt is kept constant throughout the melting interval. Variation in elemental concentrations correlate with the initial S content of the mantle source. c-e) More complex models combining melting models with K_D and SCSS functions within PySulfSat. For 200 ppm S in the mantle source, substantially different trajectories can be generated by varying the model for the amount of S in the melt, or the partition coefficient of Cu. The cyan and blue lines use a mantle melting model from Thermocalc to obtain the major element contents and temperature of instantaneous melts ([Jennings and Holland \[2015\]](#)). This allows the S content of these melts to be determined using the SCSS model of [O’Neill \[2021\]](#), assuming mantle sulfides contain 20 wt% Ni and 5 wt% Cu (after [Ding and Dasgupta \[2018\]](#)). The cyan line uses a fixed K_D for Cu (800, after [Lee et al. \[2012\]](#)). The blue line uses K_D calculated from the instantaneous silicate melt composition and an estimated mantle sulfide composition from [Kiseeva and Wood \[2015\]](#). All models assume there is 30 ppm Cu in the mantle source.

894 calculation environment. This enables a more so- 946
 895 phisticated modeling approach than existing stud- 947
 896 ies, which assumed a fixed SCSS throughout the 948
 897 melting interval (e.g., Lee et al. [2012]; Wieser et al. 949
 898 [2020]; Muth and Wallace [2022]). In reality, the 950
 899 major element composition of instantaneous melts 951
 900 will change as melting proceeds, particularly for in- 952
 901 compatible elements such as Na₂O and K₂O. Conse-
 902 quently, the SCSS will change during melting, rather
 903 than being set at a fixed value. PySulfSat can be
 904 used to calculate the SCSS for instantaneous melt
 905 compositions from melting models. For example,
 906 the cyan line in Fig. 8c-e shows calculations using
 907 instantaneous melt compositions estimated from a
 908 Thermocalc melting model (Jennings and Holland
 909 [2015]). This model using a calculated SCSS has a
 910 higher S content in the initial melts than the model
 911 assuming S=1000 ppm throughout, resulting in a
 912 lower sulfide mode, a lower bulk K_D, and thus a
 913 higher Cu concentration in mantle melts at low F
 914 values (cyan vs. dashed magenta line, Fig. 8). Sul-
 915 fide is also exhausted at a lower F (black star, part
 916 c). Changing silicate melt modes can also be used
 917 instead of a fixed modal abundance, which will cre-
 918 ate more realistic trajectories for elements with an
 919 affinity for both sulfide and silicate phases.

920 While both the cyan and magenta models on Fig.
 921 8 assume K_D for sulfide-melt is fixed at 800, Py-
 922 SulfSat can also be used to calculate K_D as a func-
 923 tion of temperature, liquid FeO content, and the Ni
 924 and Cu content of the sulfide using the model of
 925 Kiseeva and Wood [2015]. This more rigorous K_D
 926 approach results in a substantially lower K_D, and
 927 thus higher Cu contents in the melt. Additional in-
 928 formation on how to perform these more advanced
 929 melting calculations can be found at ReadTheDocs.
 930 Overall, PySulfSat gives substantially more flexibil-
 931 ity to explore concentrations in instantaneous and
 932 aggregated melts for all elements during melting in
 933 the presence of sulfide phases.

934 **9 OTHER USEFUL FUNCTIONS**

935 We also include a number of functions for other
 936 common workflows associated with S. For ex-
 937 ample, the functions `convert_d34_to_3432S` and
 938 `convert_3432S_to_d34` can be used to convert be-
 939 tween δ³⁴S values and ³⁴S/³²S ratios. By default,
 940 these functions use the the Vienna-CDT value of
 941 1/22.6436 from Ding et al. [2001], although this can
 942 be overwritten with any value of interest (using the
 943 input `st_ratio`). For example, if a dataframe is
 944 loaded in with a column for `d34S` the isotope ratio
 945 can be calculated as follows:

```
S3432=ss.convert_d34_to_3432S(d34S=df['d34S'])
```

We also include a function which allows users to en-
 ter the amount of S present in the melt as S in wt%,
 ppm, or as SO₂, SO₃, or SO₄. It then converts this
 concentration into an equivalent concentration ex-
 pressed as different species (useful when converting
 EPMA data measured as SO₂ into S in ppm for ex-
 ample):

```
df=ss.convert_S_types(S_ppm=df['S_ppm'])
```

	S_wt	S_ppm	SO2_wt	SO2_ppm	SO3_wt	SO3_ppm	SO4_wt	SO4_ppm
0	0.100	1000.0	0.199791	1997.910494	0.249687	2496.865741	0.299582	2995.820989
1	0.110	1100.0	0.219770	2197.701544	0.274655	2746.552316	0.329540	3295.403087
2	0.090	900.0	0.179812	1798.119445	0.224718	2247.179167	0.269624	2696.238890
3	0.050	500.0	0.099896	998.955247	0.124843	1248.432871	0.149791	1497.910494
4	0.040	400.0	0.079916	799.164198	0.099875	998.746297	0.119833	1198.328395
5	0.035	350.0	0.069927	699.268673	0.087390	873.903010	0.104854	1048.537346
6	0.020	200.0	0.039958	399.582099	0.049937	499.373148	0.059916	599.164198
7	0.100	1000.0	0.199791	1997.910494	0.249687	2496.865741	0.299582	2995.820989

953 Additionally, the studies of Kiseeva and Wood
 954 [2015] and Brenan [2015] parameterize K_Ds as a
 955 function of melt composition, and sulfide compo-
 956 sition for Kiseeva and Wood [2015]. The function
 957 `calculate_sulfide_kds` can be used to calculate
 958 these partition coefficients.
 959

960 **10 FUTURE WORK AND CITATION**

961 The open-source nature of PySulfSat, along with re-
 962 cent increase in interest in the behavior of S in mag-
 963 mas, means that this tool will continuously evolve.
 964 The current author team will endeavor to add new
 965 models as they are released, and anyone can submit
 966 new code using a pull request on GitHub (or by con-
 967 tacting the authors). Thus, users should check the
 968 ReadTheDocs page, where examples demonstrat-
 969 ing new functionality beyond that described in this
 970 manuscript will be added in the future. New ver-
 971 sions of PySulfSat can be obtained by running the
 972 following code in a Jupyter environment:

```
!pip install PySulfSat --upgrade
```

973 When citing calculations performed in PySulfSat in
 974 papers, users should be sure to specify which ver-
 975 sion they used, which can be obtained using:

```
ss.__version__
```

976 For example, the text may read "SCSS calculations
 977 were performed using the model of Smythe et al.
 978 [2017] implemented in PySulfSat v.1.0.3 (Wieser
 979 and Gleeson, 2023)." It is important to cite all the
 980 original papers used to perform calculations (e.g.
 981 the SCSS model, the model for S⁶⁺), as well as cit-
 982 ing PySulfSat.

983 At present, there is no open-source code that can
 984 model sulfide and sulfate saturation with all the
 985 most recent models, and the behavior of S during

986 degassing from a a silicate melt. We hope that in
987 future, the PySulfSat source code can be integrated
988 with the wide variety of S degassing tools becoming
989 available to produce a single, coherent model engine
990 for modeling S behavior in silicate melts.

991 11 REPORTING BUGS AND REQUESTING FEAT- 992 URES

993 No software is free of bugs, particularly when new
994 features are being constantly added. We have exten-
995 sively benchmarked PySulfSat to existing spread-
996 sheets, and before the package is published on PyPI,
997 automatic unit tests are run through GitHub in the
998 attempt to catch problems introduced by changing
999 Python dependencies/updates. However, if users
1000 spot any bugs, or wish to request features, they
1001 should submit an 'issue' on the GitHub page. Al-
1002 ternatively, they can email the author team.

1003 12 CONCLUSIONS

1004 PySulfSat is a open-source Python3 tool motivated
1005 by the FAIR research framework (Findable, Acces-
1006 sible, Interoperable, and Reusable). It will greatly
1007 speed up calculations, allow more inter comparison
1008 between models, and through its ease of implemen-
1009 tation with Python, allow more detailed and robust
1010 investigations of the behavior of sulfur in magmatic
1011 systems (with a rigorous consideration of errors).

1012 ACKNOWLEDGEMENTS

1013 We are grateful for help from Callum Reekie, who
1014 produced the O'Neill (2022) spreadsheet, as well as
1015 Nick Barber for motivation for this project. Thanks
1016 to Lee Saper and Ery Hughes who suggested im-
1017 plementing the method of O'Neill and Mavrogenes
1018 (2022) for calculating S^{6+}/S_T . We thank Lee Saper
1019 and Michelle Muth for very helpful reviews, We
1020 are extremely grateful for Hugh O'Neill for help-
1021 ing us understand the differences between CS6 in
1022 his paper and that of Boulliung and Wood, as well
1023 as various aspects of his S^{6+} models. Thanks to
1024 Kang Liu, Proteek Chowdhury, Julien Boulliung and
1025 Bernie Wood, Ingrid Blanchard, for providing cal-
1026 ibration data/and or spreadsheets/data to bench-
1027 mark their models. We are enormously grateful to
1028 Paula Antoshechkina for her work building Matlab
1029 and Python tools for MELTS calculations. PW was
1030 supported by UC Berkeley start up funds.

1031 AUTHOR CONTRIBUTIONS

1032 PW conceived the project, wrote the S-based code
1033 and the manuscript. MG built the fractional crys-
1034 tallization MELTS functions allowing integrating of

pyMELTScalc with PySulfSat, and contributed to
manuscript editing and code testing.

1037 DATA AVAILABILITY

1038 All files are available on GitHub (<https://github.com/PennyWieser/PySulfSat>). YouTube videos ex-
1039 plaining various aspects of the tool are avail-
1040 able on the PySulfSat YouTube channel bit.ly/PySulfSatYouTube, and Jupyter Notebook exam-
1041 ples are available on the ReadTheDocs page (bit.ly/PySulfSatRTD). The PyMELTScalc code is avail-
1042 able on GitHub ([https://github.com/gleesonm1/](https://github.com/gleesonm1/pyMELTScalc)
1043 [pyMELTScalc](https://github.com/gleesonm1/pyMELTScalc)), archived on Zenodo ([10.5281/](https://doi.org/10.5281/zenodo.7758494)
1044 [zenodo.7758494](https://doi.org/10.5281/zenodo.7758494)), and will be described in a follow
1045 up publication.

1049 REFERENCES

1050 Anenburg, M. and O'Neill, H. S. C. (2019). Redox in
1051 magmas: Comment on a recent treatment of the
1052 kaiserstuhl volcanics (braunger et al., journal of
1053 petrology, 59, 1731–1762, 2018) and some other
1054 misconceptions. *Journal of Petrology*, 60(9):1825–
1055 1832.

1056 Antoshechkina, P. M. and Ghiorso, M. S. (2018).
1057 Melts for matlab: A new educational and re-
1058 search tool for computational thermodynamics.
1059 In *AGU Fall Meeting Abstracts*, volume 2018, pages
1060 ED44B–23.

1061 Asimow, P. D. and Ghiorso, M. S. (1998). Algo-
1062 rithmic modifications extending melts to calcu-
1063 late subsolidus phase relations. *American Miner-
1064 alogist*, 83(9-10):1127–1132.

1065 Baker, D. R. and Moretti, R. (2011). Modeling the
1066 solubility of sulfur in magmas: a 50-year old geo-
1067 chemical challenge. *Reviews in Mineralogy and
1068 Geochemistry*, 73(1):167–213.

1069 Berry, A. J., Stewart, G. A., O'Neill, H. S. C., Mall-
1070 mann, G., and Mosselmans, J. F. W. (2018). A
1071 re-assessment of the oxidation state of iron in
1072 morb glasses. *Earth and Planetary Science Letters*,
1073 483:114–123.

1074 Blanchard, I., Abeykoon, S., Frost, D. J., and Ru-
1075 bie, D. C. (2021). Sulfur content at sulfide satu-
1076 ration of peridotitic melt at upper mantle condi-
1077 tions. *American Mineralogist: Journal of Earth and
1078 Planetary Materials*, 106(11):1835–1843.

1079 Borisov, A. and Shapkin, A. (1990). A new empiri-
1080 cal equation rating fe_{3+}/fe_{2+} in magmas to their
1081 composition, oxygen fugacity, and temperature.
1082 *Geochem. Int.*, 27(1):111–116.

1083 Boulliung, J. and Wood, B. J. (2022). So₂ solubility and degassing behavior in silicate melts. *Geochimica et Cosmochimica Acta*, 336:150–164. 1133

1084
1085

1086 Brenan, J. M. (2015). Se–te fractionation by sulfide–silicate melt partitioning: implications for the composition of mantle-derived magmas and their melting residues. *Earth and Planetary Science Letters*, 422:45–57. 1134

1087
1088
1089
1090

1091 Brounce, M., Stolper, E., and Eiler, J. (2017). Redox variations in mauna kea lavas, the oxygen fugacity of the hawaiian plume, and the role of volcanic gases in earth’s oxygenation. *Proceedings of the National Academy of Sciences*, 114(34):8997–9002. 1135

1092
1093
1094
1095

1096 Chowdhury, P. and Dasgupta, R. (2019). Effect of sulfate on the basaltic liquidus and sulfur concentration at anhydrite saturation (scas) of hydrous basalts—implications for sulfur cycle in subduction zones. *Chemical Geology*, 522:162–174. 1136

1097
1098
1099
1100

1101 Danyushevsky, L. V. and Plechov, P. (2011). Petrolog3: Integrated software for modeling crystallization processes. *Geochemistry, Geophysics, Geosystems*, 12(7). 1137

1102
1103
1104

1105 Ding, S. and Dasgupta, R. (2018). Sulfur inventory of ocean island basalt source regions constrained by modeling the fate of sulfide during decompression melting of a heterogeneous mantle. *Journal of Petrology*, 59(7):1281–1308. 1138

1106
1107
1108
1109

1110 Ding, T., Valkiers, S., Kipphardt, H., De Bievre, P., Taylor, P., Gonfiantini, R., and Krouse, R. (2001). Calibrated sulfur isotope abundance ratios of three iaea sulfur isotope reference materials and v-cdt with a reassessment of the atomic weight of sulfur. *Geochimica et Cosmochimica Acta*, 65(15):2433–2437. 1139

1111
1112
1113
1114
1115
1116

1117 Edmonds, M., Mather, T. A., and Liu, E. J. (2018). A distinct metal fingerprint in arc volcanic emissions. *Nature Geoscience*, 11(10):790–794. 1140

1118
1119

1120 Fincham, C. and Richardson, F. D. (1954). The behaviour of sulphur in silicate and aluminate melts. *Proceedings of the Royal Society of London. Series A. Mathematical and Physical Sciences*, 223(1152):40–62. 1141

1121
1122
1123
1124

1125 Fortin, M.-A., Riddle, J., Desjardins-Langlais, Y., and Baker, D. R. (2015). The effect of water on the sulfur concentration at sulfide saturation (scss) in natural melts. *Geochimica et Cosmochimica Acta*, 160:100–116. 1142

1126
1127
1128
1129

1130 Frost, B. (1991). Chapter 1. introduction to oxygen fugacity and its petrological importance. *Oxide minerals*, pages 1–10. 1143

1131
1132

Ghiorso, M. S. and Sack, R. O. (1995). Chemical mass transfer in magmatic processes iv. a revised and internally consistent thermodynamic model for the interpolation and extrapolation of liquid–solid equilibria in magmatic systems at elevated temperatures and pressures. *Contributions to Mineralogy and Petrology*, 119(2):197–212. 1144

1140
1141
1142
1143

Gleeson, M., Paula, A., and Wieser, P. (2023). Pymeltscalc. *GitHub* - <https://github.com/gleesonm1/pyMELTScalc>, 10.5281/zenodo.7758494. 1145

1144
1145
1146
1147
1148

Gualda, G. A. and Ghiorso, M. S. (2015). Melts _ excel: An microsoft excel-based melts interface for research and teaching of magma properties and evolution. *Geochemistry, Geophysics, Geosystems*, 16(1):315–324. 1149

1149
1150
1151
1152
1153

Gualda, G. A., Ghiorso, M. S., Lemons, R. V., and Carley, T. L. (2012). Rhyolite-melts: a modified calibration of melts optimized for silica-rich, fluid-bearing magmatic systems. *Journal of Petrology*, 53(5):875–890. 1154

1154
1155
1156
1157
1158

Harris, C. R., Millman, K. J., van der Walt, S. J., Gommers, R., Virtanen, P., Cournapeau, D., Wieser, E., Taylor, J., Berg, S., Smith, N. J., et al. (2020). Array programming with numpy. *Nature*, 585(7825):357–362. 1159

1159
1160
1161

Hunter, J. D. (2007). Matplotlib: A 2d graphics environment. *Computing in Science & Engineering*, 9(3):90–95. 1162

1162
1163
1164
1165
1166

Iacono-Marziano, G., Le Vaillant, M., Godel, B. M., Barnes, S. J., and Arbaret, L. (2022). The critical role of magma degassing in sulphide melt mobility and metal enrichment. *Nature Communications*, 13(1):2359. 1167

1167
1168
1169
1170

Jennings, E. S. and Holland, T. J. (2015). A simple thermodynamic model for melting of peridotite in the system ncfmasocr. *Journal of Petrology*, 56(5):869–892. 1171

1171
1172
1173
1174
1175

Johnson, C. M., Ghiorso, M. S., Spiegelman, M., Wolf, A. S., Adams, J., and Myhill, R. (2022). Thermoengine: Thermodynamic properties estimator and phase equilibrium calculator. *Astrophysics Source Code Library*, pages ascl–2208. 1176

1176
1177

Jugo, P. J. (2009). Sulfur content at sulfide saturation in oxidized magmas. *Geology*, 37(5):415–418. 1178

1178
1179
1180
1181
1182
1183

Jugo, P. J., Wilke, M., and Botcharnikov, R. E. (2010). Sulfur k-edge xanes analysis of natural and synthetic basaltic glasses: Implications for s speciation and s content as function of oxygen fugacity. *Geochimica et Cosmochimica Acta*, 74(20):5926–5938. 1184

- 1184 Kilinc, A., Carmichael, I., Rivers, M. L., and Sack, R. O. (1983). The ferric-ferrous ratio of natural silicate liquids equilibrated in air. *Contributions to Mineralogy and Petrology*, 83(1-2):136–140. 1237
- 1185
1186
1187
- 1188 Kiseeva, E. S. and Wood, B. J. (2015). The effects of composition and temperature on chalcophile and lithophile element partitioning into magmatic sulphides. *Earth and Planetary Science Letters*, 424:280–294. 1241
- 1189
1190
1191
1192
- 1193 Kleinsasser, J. M., Simon, A. C., Konecke, B. A., Kleinsasser, M. J., Beckmann, P., and Holtz, F. (2022). Sulfide and sulfate saturation of dacitic melts as a function of oxygen fugacity. *Geochimica et Cosmochimica Acta*, 326:1–16. 1242
- 1194
1195
1196
1197
- 1198 Kress, V. C. and Carmichael, I. S. (1988). Stoichiometry of the iron oxidation reaction in silicate melts. *American Mineralogist*, 73(11-12):1267–1274. 1243
- 1199
1200
1201
- 1202 Lee, C.-T. A., Luffi, P., Chin, E. J., Bouchet, R., Dasgupta, R., Morton, D. M., Le Roux, V., Yin, Q.-z., and Jin, D. (2012). Copper systematics in arc magmas and implications for crust-mantle differentiation. *Science*, 336(6077):64–68. 1244
- 1203
1204
1205
1206
- 1207 Lerner, A. H., Muth, M. J., Wallace, P. J., Lanzirotti, A., Newville, M., Gaetani, G. A., Chowdhury, P., and Dasgupta, R. (2021). Improving the reliability of Fe and S XANES measurements in silicate glasses: Correcting beam damage and identifying Fe-oxide nanolites in hydrous and anhydrous melt inclusions. *Chemical Geology*, 586:120610. 1245
- 1208
1209
1210
1211
1212
1213
- 1214 Li, C. and Ripley, E. M. (2009). Sulfur contents at sulfide-liquid or anhydrite saturation in silicate melts: empirical equations and example applications. *Economic Geology*, 104(3):405–412. 1246
- 1215
1216
1217
- 1218 Li, H. and Zhang, L. (2022). A thermodynamic model for sulfur content at sulfide saturation (scss) in hydrous silicate melts: With implications for arc magma genesis and sulfur recycling. *Geochimica et Cosmochimica Acta*, 325:187–204. 1247
- 1219
1220
1221
1222
- 1223 Liu, K., Zhang, L., Guo, X., and Ni, H. (2021). Effects of sulfide composition and melt H₂O on sulfur content at sulfide saturation in basaltic melts. *Chemical Geology*, 559:119913. 1248
- 1224
1225
1226
- 1227 Mason, E., Wieser, P. E., Liu, E. J., Edmonds, M., Ilyinskaya, E., Whitty, R. C., Mather, T. A., Elias, T., Nadeau, P. A., Wilkes, T. C., et al. (2021). Volatile metal emissions from volcanic degassing and lava-seawater interactions at Kīlauea volcano, Hawai‘i. *Communications Earth & Environment*, 2(1):1–16. 1249
- 1228
1229
1230
1231
1232
1233
- 1234 Masotta, M. and Keppler, H. (2015). Anhydrite solubility in differentiated arc magmas. *Geochimica et Cosmochimica Acta*, 158:79–102. 1250
- 1235
1236
- Muth, M. J. and Wallace, P. J. (2021). Slab-derived sulfate generates oxidized basaltic magmas in the southern cascade arc (California, USA). *Geology*, 49(10):1177–1181. 1240
- Muth, M. J. and Wallace, P. J. (2022). Sulfur recycling in subduction zones and the oxygen fugacity of mafic arc magmas. *Earth and Planetary Science Letters*, 599:117836. 1241
- Myers, J. T. and Eugster, H. (1983). The system Fe-Si-O: Oxygen buffer calibrations to 1,500 K. *Contributions to Mineralogy and Petrology*, 82:75–90. 1242
- Myers, J. T. and Eugster, H. (1983). The system Fe-Si-O: Oxygen buffer calibrations to 1,500 K. *Contributions to Mineralogy and Petrology*, 82:75–90. 1243
- Nash, W. M., Smythe, D. J., and Wood, B. J. (2019). Compositional and temperature effects on sulfur speciation and solubility in silicate melts. *Earth and Planetary Science Letters*, 507:187–198. 1244
- Nash, W. M., Smythe, D. J., and Wood, B. J. (2019). Compositional and temperature effects on sulfur speciation and solubility in silicate melts. *Earth and Planetary Science Letters*, 507:187–198. 1245
- O’Neill, H. S. (1987). Quartz-fayalite-iron and quartz-fayalite-magnetite equilibria and the free energy of formation of fayalite (Fe₂SiO₄) and magnetite (Fe₃O₄). *American Mineralogist*, 72(1-2):67–75. 1246
- O’Neill, H. S. (1987). Quartz-fayalite-iron and quartz-fayalite-magnetite equilibria and the free energy of formation of fayalite (Fe₂SiO₄) and magnetite (Fe₃O₄). *American Mineralogist*, 72(1-2):67–75. 1247
- O’Neill, H. S. C. (2021). The thermodynamic controls on sulfide saturation in silicate melts with application to ocean floor basalts. *Magma Redox Geochemistry*, pages 177–213. 1248
- O’Neill, H. S. C., Berry, A. J., and Mallmann, G. (2018). The oxidation state of iron in mid-ocean ridge basaltic (morb) glasses: Implications for their petrogenesis and oxygen fugacities. *Earth and Planetary Science Letters*, 504:152–162. 1249
- O’Neill, H. S. C. and Mavrogenes, J. A. (2022). The sulfate capacities of silicate melts. *Geochimica et Cosmochimica Acta*, 334:368–382. 1250
- O’Neill, H. S. C. and Mavrogenes, J. A. (2022). The sulfate capacities of silicate melts. *Geochimica et Cosmochimica Acta*, 334:368–382. 1251
- pandas development team, T. (2020). pandas-dev/pandas: Pandas. 1252
- Putirka, K. (2016). Rates and styles of planetary cooling on Earth, Moon, Mars, and Vesta, using new models for oxygen fugacity, ferric-ferrous ratios, olivine-liquid Fe-Mg exchange, and mantle potential temperature. *American Mineralogist*, 101(4):819–840. 1253
- Putirka, K. (2016). Rates and styles of planetary cooling on earth, moon, mars, and vesta, using new models for oxygen fugacity, ferric-ferrous ratios, olivine-liquid fe-mg exchange, and mantle potential temperature. *American Mineralogist*, 101(4):819–840. 1254
- Reekie, C., Jenner, F., Smythe, D., Hauri, E., Bullock, E., and Williams, H. (2019). Sulfide resorption during crustal ascent and degassing of oceanic plateau basalts. *Nature communications*, 10(1):1–11. 1255
- Reekie, C., Jenner, F., Smythe, D., Hauri, E., Bullock, E., and Williams, H. (2019). Sulfide resorption during crustal ascent and degassing of oceanic plateau basalts. *Nature communications*, 10(1):1–11. 1256
- Sack, R., Carmichael, I., Rivers, M., and Ghiorso, M. (1981). Ferric-ferrous equilibria in natural silicate liquids at 1 bar. *Contributions to Mineralogy and Petrology*, 75:369–376. 1257
- Sack, R., Carmichael, I., Rivers, M., and Ghiorso, M. (1981). Ferric-ferrous equilibria in natural silicate liquids at 1 bar. *Contributions to Mineralogy and Petrology*, 75:369–376. 1258
- Sack, R., Carmichael, I., Rivers, M., and Ghiorso, M. (1981). Ferric-ferrous equilibria in natural silicate liquids at 1 bar. *Contributions to Mineralogy and Petrology*, 75:369–376. 1259
- Sack, R., Carmichael, I., Rivers, M., and Ghiorso, M. (1981). Ferric-ferrous equilibria in natural silicate liquids at 1 bar. *Contributions to Mineralogy and Petrology*, 75:369–376. 1260

- 1289 Smythe, D. J., Wood, B. J., and Kiseeva, E. S. (2017). 1286
 1290 The s content of silicate melts at sulfide saturation: new experiments and a model incorporating 1287
 1291 the effects of sulfide composition. *American Mineralogist*, 102(4):795–803. 1288
- 1291 Virtanen, P., Gommers, R., Oliphant, T. E., Haberland, M., Reddy, T., Cournapeau, D., Burovski, E., Peterson, P., Weckesser, W., Bright, J., van der Walt, S. J., Brett, M., Wilson, J., Millman, K. J., Mayorov, N., Nelson, A. R. J., Jones, E., Kern, R., Larson, E., Carey, C. J., Polat, İ., Feng, Y., Moore, E. W., VanderPlas, J., Laxalde, D., Perktold, J., Cimrman, R., Henriksen, I., Quintero, E. A., Harris, C. R., Archibald, A. M., Ribeiro, A. H., Pedregosa, F., van Mulbregt, P., and SciPy 1.0 Contributors (2020). SciPy 1.0: Fundamental Algorithms for Scientific Computing in Python. *Nature Methods*, 17:261–272.
- 1304 Virtanen, V. J., Heinonen, J. S., Barber, N. D., and Molnár, F. (2022). Complex effects of assimilation on sulfide saturation revealed by modeling with the magma chamber simulator: A case study on the duluth complex, minnesota, usa. *Economic Geology*.
- 1310 Wallace, P. J. and Carmichael, I. S. (1994). S speciation in submarine basaltic glasses as determined by measurements of s $\kappa\alpha$ x-ray wavelength shifts. *American Mineralogist*, 79(1-2):161–167.
- 1314 Wieser, P. and Jenner, F. (2021). Chalcophile elements: Systematics and relevance. *Reference Module in Earth Systems and Environmental Sciences*, pages 67–80.
- 1318 Wieser, P., Petrelli, M., Lubbers, J., Wieser, E., Ozaydin, S., Kent, A., and Till, C. (2022). Thermobar: an open-source python3 tool for thermobarometry and hygrometry. *Volcanica*, 5(2):349–384.
- 1322 Wieser, P. E., Jenner, F., Edmonds, M., Maclennan, J., and Kunz, B. E. (2020). Chalcophile elements track the fate of sulfur at kilauea volcano, hawai'i. *Geochimica et Cosmochimica Acta*, 282:245–275.
- 1326 Zajacz, Z. and Tsay, A. (2019). An accurate model to predict sulfur concentration at anhydrite saturation in silicate melts. *Geochimica et Cosmochimica Acta*, 261:288–304.